NASA Contractor Report 177543

Application of the Joined Wing to Tiltrotor Aircraft

Julian Wolkovitch, Barnaby Wainfan,
Yitzhak Ben-Harush, and Wayne Johnson

CONTRACT NAS2–12988
November 1989

National Aeronautics and
Space Administration

NASA Contractor Report 177543

Application of the Joined Wing to Tiltrotor Aircraft

Julian Wolkovitch, Barnaby Wainfan,
and Yitzhak Ben-Harush
ACA Industries, Inc., Rancho Palos Verdes, California

Wayne Johnson
Johnson Aeronautics, Palo Alto, California

Prepared for
Ames Research Center
CONTRACT NAS2–12988
November 1989

National Aeronautics and
Space Administration

Ames Research Center
Moffett Field, California 94035

TABLE OF CONTENTS

LIST OF TABLES

FIGURES

PROJECT SUMMARY

A study was made to determine the potential speed improvements and other benefits resulting from the application of the joined wing concept to tiltrotor aircraft. Using the XV-15 as a baseline, the effect of replacing the cantilever wing by a joined-wing pair was studied. The baseline XV-15 cantilever wing has a thickness/chord ratio of 23%. It was found that this wing could be replaced by a joined-wing pair of the same span and total area employing airfoils of 12% thickness/chord ratio. The joined wing meets the same static strength requirements as the cantilever wing, but increases the limiting Mach Number of the aircraft from M= 0.575 to M= 0.75, equivalent to an increase of over 100 knots in maximum speed.

The joined wing configuration studied is lighter than the cantilever and has approximately 11% less wing drag in cruise. Its flutter speed of 245 knots EAS is not high enough to allow the potential Mach number improvement to be attained at low altitude. The flutter speed can be raised either by employing rotors which can be stopped and folded in flight at speeds below 245 knots EAS, or by modifying the airframe to reduce adverse coupling with the rotor dynamics. Several modifications of wing geometry and nacelle mass distribution were investigated, but none produced a flutter speed above 260 knots EAS. It was concluded that additional research is required to acieve a more complete understanding of the mechanism of rotor/wing coupling, and to implement improvements through changes in wing geometry, advanced materials, or rotor modifications.

If the flutter speed can be raised, the research would yield increases in speed of tiltrotor aircraft, enabling such aircraft to combine their vertical takeoff and landing capabilities with cruise speeds equal to those of conventional aircraft.

1.0. INTRODUCTION

1.1 OBJECTIVE OF THE PRESENT STUDY

The principal objective of the study reported here is to investigate the feasibility of combining two promising aircraft configuration concepts: the joined wing and the tiltrotor. Each of these concepts can take many different forms. For example, the joined wing may have the interwing joint located either at the tips or inboard, as shown in Figs. 1 and 2. The tiltrotor may employ fully tilting nacelles, as on the XV-15 (Fig. 3), or fixed nacelles and tilting shafts (Fig. 4). Figure 5 shows yet another variant of the tiltrotor concept, the folding tiltrotor. This employs stoppable folding rotors to eliminate the forward speed limitations of rotors.

All of the above approaches to tiltrotor design share the principal goal of the tiltrotor concept: to achieve the cruise speed of a fixed-wing aircraft while retaining the hover capability of a helicopter. The present study explores how the joined wing concept may be applied to reach this goal.

1.2 ORGANIZATION OF THIS REPORT

A brief description of the fundamentals of the joined wing is given in Section 1.3. Section 1.4 reviews problems and limitations of current tiltrotors. These include: (1) structural requirements for thick airfoils, with typical thickness/chord ratios of 23%, which develop compressibility drag at low Mach Numbers, (2) aeroelastic wing/rotor coupling causing low flutter speeds, (3) hover thrust losses due to the wing being immersed in the rotor downwash, and (4) rotor/wing aerodynamic interference in cruise, causing reduced propulsive efficiency and increased

vibration. Section 1.5 describes the main topic of the initial study effort, i.e. the use of the joined wing to permit thinner airfoils having increased Mach Number capabilities. In particular, the maximum speed and the aeroelastic behavior of tiltrotor aircraft having joined wings with 12% to 15 % thick airfoils was selected for investigation.

Section 2 presents data on the XV-15, which is used as a baseline reference aircraft. The computer program methods used in the present study to compute flutter speeds (MSC-PAL and CAMRAD) are validated by comparing their predictions of XV-15 aeroelastic characteristics against published predictions based on NASTRAN models, and also with data from ground vibration tests and in-flight measurements.

Section 3 describes the static structural design considerations of joined wing tiltrotors. It is shown that the 23% thick XV-15 wing can be replaced by a joined-wing pair with front and rear wings each 12% thick, while still meeting the design strength criteria, at no increase in structural weight.

Section 4 outlines the potential performance gains of such thin joined wings, and also discusses their integration with the rest of the configuration. Practical design implications such as rotor clearance, fuel volume, cross-shafting accommodation are discussed. It is shown that the reduction in wing thickness opens up the possibility of large gains in maximum Mach Number, equivalent to an increase in True Air Speed of over 100 knots.

Section 5 presents predictions of aeroelastic characteristics and whirl flutter speeds. If folding rotors are used, the flutter speed must exceed the speed at which the rotors are stopped and folded. It is shown that this condition can be satisfied by a wide range of joined wings with 12% thick airfoils. However, for nonfolding rotors, the whirl flutter

speed must exceed the maximum Mach Number capability of the aircraft. This requirement was found to restrict the allowable joined wing geometries and mass distributions. It is shown that the distribution of nacelle mass, and the front wing sweep angle critically influence flutter speed.

Section 6 discusses approaches to developing rotor/wing combinations having flutter speeds to match the increased Mach Number capabilities of the thin joined wings.

Conclusions, and recommendations for further work are given in Section 7.

1.3. THE JOINED WING: A BRIEF SUMMARY

A complete survey of the joined wing has been given in Ref. 1, so only the points of special interest to tiltrotors are listed here. It has been shown that, compared to a conventional wing-plus-tail of the same span and total area made from the same material and carrying the same load, a joined wing can have the following advantages:

1. LIGHTER by as much as 42%.

2. STIFFER; e.g 26% increase in flutter speed

3. SUITABLE FOR THINNER AIRFOILS WITH LESS WEIGHT PENALTY

4. HIGHER SPAN-EFFICIENCY FACTOR, e.g. 9% less induced drag.

Folding models have been constructed showing that joined wings can be folded without separating the tip joint. No fundamental stability and control deficiencies have been found in any of the eight different wind-tunnel models that have been tested since 1979.

To achieve the lightest possible joined wing, it is generally necessary to distribute the wing structural materialdifferently from a cantilever wing. As shown in Fig. 6, this involves distributing the structural material at any given spanwise station such that the principal axis of the second moment of area is tilted with respect to the chord line. The optimum tilt angle generally varies along the span.

Although most published examples of joined wings show the rear wing located higher than the front wing, the wings can be reversed, so that the rear wing is lower. The front and rear

wings need not have sweep angles of opposite sign. Several tiltrotor configurations presented later in this report employ forward sweep on both the front and rear wings.

1.4 TILTROTOR PROBLEMS AND LIMITATIONS

Although several successful tiltrotor aircraft have flown, certain problems remain which are fundamental to the tiltrotor concept. Some of these significantly impact performance. The following are particularly important:

1: THICK AIRFOILS: Current tiltrotor aircraft employ very thick airfoils to obtain adequate wing stiffness and strength to handle the loads imposed by vertical-jump takeoffs. Both the V-22 and the XV-15 use wing airfoils with a thickness/chord ratio of 23%. Such thick airfoils prevent the tiltrotor concept from achieving its high-speed potential. The XV-15 is limited by wing compressibility effects to M = 0.575, equivalent to approximately 300 KEAS or 360 KTAS at 12,000 ft. The V-22 limit is similar.

2: AEROELASTIC WING/ROTOR COUPLING: Tiltrotor aircraft are susceptible to an aeroelastic instability known as whirl flutter, typically involving coupling of rotor in-plane forces with wing flapping and nacelle pitching (Ref. 2). The speed for whirl flutter must exceed by a sufficient margin the maximum speed of the aircraft determined by thrust = drag. To achieve this margin it may be necessary to increase wing stiffness by adding extra structural material (leading to increased weight). Alternatively, external bracing struts can be employed, as was done on the XV-3 and Bell-Boeing Pointer, at the cost of increased drag.

3: HOVER THRUST LOSSES: Felker and Light (Ref. 3) show that the net hover thrust of tiltrotor aircraft is typically

11 % less than the isolated thrust of the rotors at the given shaft power. This thrust loss seriously degrades the load-carrying capability of the vehicle. It is caused by two phenomena, as illustrated in Fig. 7. One is the direct drag (download) of the wings, the other is the recirculation or fountain effect occurring near the aircraft plane of symmetry.

4. ROTOR-WING INTERFERENCE IN CRUISE: Current tiltrotors employ thick, large-chord wings having leading edges located only a short distance aft of the rotor (typically 0.25 times rotor radius). Thus each blade cycles through the wing upwash field at 1 per rev. This reduces propulsive efficiency and increases vibratory loads on the wing. The problem could be alleviated by moving the rotor further ahead of the wing, but this would require increasing rotor mast height. This is undesirable because it tends to reduce the speed at which whirl flutter will occur.

Considering the above problems of thick airfoils, aeroelastic wing/rotor coupling, hover thrust losses, and rotor/wing aerodynamic interference in cruise, it is clear that there are several different ways in which the joined wing could be applied to benefit tiltrotors. For example, Fig. 8 shows a joined wing configuration with wings that are superimposed in plan view. This configuration presents a minimal projected area to the rotor downwash in hover, possibly reducing the hover thrust loss. On the other hand, the close proximity of the unstaggered wing tips would demand careful airfoil design to avoid inducing compressibility drag at too low a Mach Number.

1.5 SPECIFIC TECHNICAL APPROACH

The scope of the present study did not permit all of the above problems to be tackled. It was decided that the highest priority should be given to Problems 1 and 2, i.e. raising maximum Mach Number and increasing whirl flutter speed. The value of achieving these goals has been delineated by Johnson, Lau and Bowles (Ref. 4). This reference shows that, at 400 knots, V-22 wing and rotor compressibility effects would each absorb approximately 10% of the total power. Using thinner airfoils at no change in weight would eliminate compressibility drag at 400 knots, reducing cruise power by approximately 10%. Eliminating the wing compressibility drag with no structural weight penalty saves fuel. The reduction in fuel weight for a given mission reduces hover thrust and power requirements, thus reducing the size and weight of the required engines and transmission. The compounded effect of eliminating wing compressibility drag is large. Reference 4 states that it can lead to a reduction in gross weight of 10%. The above results support the decision to focus the present study on increasing the Mach Number limits and raising flutter speed.

The approach taken was to start with the XV-15, as a well-documented baseline aircraft, and to modify it by replacing the existing 23% cantilever wing with a joined wing pair of the same span and total area. The cruise performance and maximum speed were compared, and whirl flutter speeds calculated. A series of variations in wing sweep angle and nacelle geometry were explored to determine the parametric effects of these variables on flutter speed.

2.0 BASELINE CONFIGURATION AND VALIDATION OF TECHNICAL APPROACH

2.1 XV-15 GEOMETRIC DATA

Figure 9 shows the XV-15 aircraft. This was selected as a baseline configuration because the design and performance of the aircraft are well documented and a large body of data exists comparing theoretical and experimental characteristics. Reference 5 contains a comprehensive summary of the geometric and performance characteristics of the XV-15.

Some geometric features that deserve special note are the airfoil thickness/chord ratios, which are 23% on the wing and 15% on the horizontal tail. The design flapping clearance allows the rotor blades to flap between +12 and -12 degrees from a precone angle of 2.5 degrees. At -12 degrees flapping the clearance between the rotor tip and the wing leading edge is 0.47 ft. Also note that the wing and the cross-shafting are not straight; both have -6.5 degrees sweep, and 2 degrees dihedral. The rotor shafts are parallel in cruise, but are toed out 2.5 degrees in hover.

Table 1 presents a weight breakdown, with 242 lb of fuel removed to bring the gross weight to its design value of 13,000 lb.

The structural characteristics of the XV-15 wing were estimated from Ref. 6, from which Fig. 10 was obtained. This shows the spanwise distribution of bending stiffness EI, torsional stiffness GJ, and mass (including fuel) for the XV-15 wing.

2.2 VALIDATION OF ANALYSIS METHODS EMPLOYED

For general-purpose structural analyses, the MSC-PAL finite element program was employed. This was used in conjunction with the data of Fig. 10 to compute mode shapes and frequencies for the baseline XV-15. Each wing was modeled by 4 elements, and simple stick models were used for the rest of the structure as shown in Fig. 11, and Table 2. The results were compared with those of a more complex NASTRAN model and with experimental data from ground vibration tests. Table 3 illustrates this comparison. The agreement is good for the low frequency modes, which are the modes of primary interest for flutter calculations, as will be shown.

The CAMRAD program developed by Dr. Wayne Johnson (Refs. 7,8, 9, 10) was employed to calculate flutter speeds. CAMRAD (Comprehensive Analytical Model for Rotorcraft Aerodynamics and Dynamics) provides trim solutions and rigid and elastic flight dynamics, including coupling between rotor flapping and inplane motions and wing torsion and bending parallel to both chordwise and vertical axes. CAMRAD has been validated against XV-15 test data (Ref. 11), and V-22 model test data (Ref. 2). The CAMRAD results were close to the measured data for both aircraft. These validations indicate that CAMRAD should be accurate for joined-wing tiltrotors, provided it is supplied with accurate structural data.

CAMRAD requires as input the mode shapes and frequencies of the tiltrotor structure measured at the rotor hub. Table 5 shows these quantities calculated for the XV-15 MSC-PAL model for the starboard rotor hub.

Each joined wing structure analyzed here was designed to meet the same stressing criteria as the XV-15. Figure 12 shows the XV-15 flight envelope. Reference 6 notes that the most

severe wing bending moments were obtained from the jump vertical take-off condition, which is a 2 g maneuver with a 1.5 factor of safety.

The structural members of the joined wing structure were sized by means of the JAWS program. JAWS (Joined Analysis of Wing Structures), developed by ACA Industries, Inc., computes loads and stresses in joined wings. It is a static structural analysis program specialized for joined wings and requiring only a few key parameters as input. These include span, root and tip chord, dihedral, sweep, airfoil ordinates, and skin thickness distribution for the front and rear wings. The program includes beam-column effects, which as explained in Ref. 1, can be significant for joined wings. JAWS has been validated against other finite-element programs and against proof-load tests on the full-scale joined-wing Unmanned Air Vehicle described in Ref. 12.

2.3 TECHNICAL STUDY PROCEDURE

The procedure for comparing various joined-wing configurations with the baseline XV-15 was as follows.

(1) Replace the cantilever wing by a joined wing selected to match the operational requirements of the baseline aircraft. The structural design of the joined wing is carried out using the JAWS program.

(2) Compute the relative lifting surface weights of the baseline cantilever and the joined wing versions, using published data for the XV-15, and the results of the JAWS program (which can predict weights of cantilever as well as joined wings).

(3) Compute mode shapes and frequencies for both the cantilever and joined-wing versions, by standard finite-element methods, and input the results to CAMRAD. Compare the flutter boundaries and other dynamic characteristics of the baseline and the joined-wing vehicles.

(4) From the results of (a) through (d), plan further investigations.

3.0 DEVELOPMENT OF JOINED-WING TILTROTOR CONFIGURATION

3.1. GENERAL CONSIDERATIONS

The primary objective of the current study was to employ the joined wing to maximize the speed potential of the aircraft. Unlike most propeller-driven airplanes which are limited by propeller Mach-Number effects, the XV-15 and V-22 are both limited to relatively low maximum Mach Numbers by the compressible-flow characteristics of the very thick wings they employ to meet structural requirements. By using the joined wing to reduce the thickness-to-chord ratio of the wing airfoils, while meeting structural requirements, the limiting Mach Number of the wing can be substantially increased. The limiting factors for a simple tiltrotor vehicle then become proprotor Mach Number effects rather than wing critical Mach Number. When employed in combination with folding proprotors, the thinner joined wing allows the vehicle to fly much faster than the thick, cantilever-winged vehicle. As noted in Ref.6, the static loads during a vertical-jump takeoff size the wing structure. Hence, stopping the rotors in cruise will not allow the wing of a cantilever tiltrotor to be any thinner and will not raise the aircraft's Mach number limits set by drag divergence and shock stall.

A further aspect to be considered in selecting the best joined-wing configuration for the mission is structural weight of the lifting surfaces. This represents dead weight, which subtracts from potential payload. Minimizing the lifting surface total weight reduces hover power, and hence compounds the weight saving. In selecting the joined wing thickness/chord ratio a trade-off must be made between saving weight and increasing speed capability. In the current study, emphasis was placed on increasing speed potential rather than weight reduction. It was, however, stipulated that the joined-wing configuration flying-surface weight be no greater that of the XV-15.

3.2 JOINED-WING CONFIGURATIONS

Figure 13 shows Configuration 166-AL, which was used as a starting point for the analysis of joined-wing tiltrotors. The fuselage, tail and nacelles of this configuration are assumed to have the same external geometry and mass as the corresponding components of the XV-15. The XV-15 wing is replaced by a joined wing pair of the same span and total area as the XV-15 wing. The front wing chord is twice that of the rear wing. The ratio of flap chord to wing chord is the same as for the cantilever wing. Hence when the flaps are drooped the wing area normal to the slipstream is the same for the joined and cantilever configurations. Thus the hover download losses should not be worse for the joined wing than for the cantilever configuration.

A significant difference between Configuration 166-AL and the XV-15 is that the joined front and rear airfoils both have NACA 64212 airfoils with thickness/chord ratios of 12%, whereas the XV-15 wing is 23% thick.

Table 4 lists the principal configurations analyzed. All the configurations retained the fuselage and tail of the XV-15. The effects of varying the following parameters were studied:

(1) front and/or rear wing sweep angles
(2) front wing thickness/chord ratio
(3) nacelle geometry and mass distribution

The nacelle design perturbations were done to improve the structural dynamics of the wings, as described in Section 5, and did not affect the static strength characteristics discussed in the present Section.

3.3. STRUCTURAL DESIGN FOR STATIC LOADING

From manufacturer's design data the critical loading case was determined to be a maximum-gross-weight, vertical-jump takeoff. Accordingly, the wings were designed to withstand a 2-g loading imposed by vertical forces at the tips along with the propulsion-system torques transmitted through the nacelles. A factor of safety of 1.5 was used, yielding an ultimate load factor of 3.0. The wing structure was designed to be made of aluminum alloy. All static structural design and weight analyses were performed using a version of ACA's JAWS code adapted specially for tilt-rotor applications.

Initially, it was decided to hold the leading-edge sweep of the front wing at -6.5 degrees which is the leading-edge sweep of the baseline XV-15 wing. A limited investigation of the effects of rear-wing sweep was done. Plan views of the configurations considered are shown in Fig. 14. The configuration with 30 degrees of rear-wing sweep was thought to be aeroelastically desirable because of its high bending stiffness about the Z axis. However, detailed JAWS analysis of this configuration showed that, under the specified 2g jump-takeoff loading, a rear wing having 30 degrees of forward sweep imposes an excessively large compression load on the front wing. The resulting penalty in front wing weight negated the benefit of increased chordwise stiffness, and so this configuration was not studied further.

Analysis of the 6.5-degree-forward-sweep rear wing configuration showed that it offered no weight advantage over the 15-degree-forward-sweep configuration and had a lower flutter boundary.

The selected joined-wing tiltrotor configuration of Fig. 13 has 15 degrees of rear-wing sweep and 23 degrees of rear-wing dihedral and appeared to offer a reasonable compromise between aeroelastic and static-load requirements.

3.4. CONFIGURATION EFFECTS ON WING WEIGHT

Aeroelastic considerations dictated that additional combinations of front and rear wing sweep be considered. A list of these configurations can be found in Table 4. The primary impact of wing-sweep changes on the static-load structural design was changes in wing weight. In general, the wing weight correlated with the stagger of the wings at the root. The larger the stagger, the heavier the wing set. From a static-load minimum-weight point of view, the configurations with the least stagger are superior.

The present study concentrated on using the joined wing to reduce the thickness-to-chord ratio of the wing in order to increase speed potential. Thus, the potential wing-weight saving which could have been achieved with a joined wing having aerodynamic limitations similar to the baseline cantilever wing it replaces was not investigated.

From manufacturers's estimates, the complete structure weight of the baseline 23-percent-thick XV-15 wing is 946 lb. (Various sources give slightly different weights, but the above weight is based on the most detailed weight breakdown available to us, and we believe it is accurate.) The 12-percent-thick joined-wing tiltrotor configuration 166-AL is computed by the JAWS program to weigh 858 pounds. The weights of the other sweep, stagger and thickness combinations investigated can be found in Table 4. In comparing the weights estimated by the JAWS program for joined wings versus cantilever wings it should be

noted that (1) the joined wing weights do not include an allowance for flaps, and (2) the JAWS finite-element model employs a relatively coarse grid. These two effects approximately cancel, and the relative weights of the joined and cantilever configurations are believed to be compared on a fair basis. No credit for wing weight saved was taken in computing gross weight: both the cantilever and joined wing configurations were assumed to weigh 13,000 lb (except where otherwise noted).

The joined wing enables the thickness-to-chord ratio of the wing to be cut almost in half, while wing weight remains the same or smaller than the baseline cantilever wing. The primary reason for this is illustrated in Figures 15 and 16 which show comparisons of the bending moments acting on the wings in the Y-Z (rolling) plane and X-Y (yawing) plane during a 3-G vertical-jump takeoff at a gross weight of 13,000 pounds. Note, in particular, that the bending moment about the X axis is reduced by an order of magnitude for the joined wing.

(The Y-Z and X-Y planes referred to above are not exactly body-axis rolling and yawing planes. They refer to individual orthognal axis systems Oxyz for each wing, with the origin at the intersection of that particular wing's 40% chordline and the aircraft plane of symmetry. The y-axis points to starboard along the 40% chordline, the x-axis points aft along the root chordline, and the z-axis points upward normal to the Oxy plane. In the configurations studied here the location of the tip leading edge of each front joined wing was identical to that of the XV-15 tip leading edge. The sweep angle variations studied in the present report did not involve any change in wing chords. Hence, although the root chord of each wing was displaced by changes in sweep angle, the tip remained in the same location.)

The joined wings analysed here did not exploit the full potential of the joined wing to save weight because, for ease of

computation, the principal inertia axis of the wing structure was assumed to be parallel to the chord line, and not tilted as in Fig. 6. Lighter joined wings could be achieved with a more refined distribution of structural material. Similarly, since the aerodynamic center of the joined wing is aft of that of the cantilever baseline there exists some potential to reduce horizontal tail area and thus save further weight. However, since light weight was not the principal goal of the study, these and other weight-saving opportunities were not explored. It was verified however, that each joined wing configuration presented here is at least no heavier than the baseline configuration.

4.0 CRUISE PERFORMANCE, STABILITY AND CONTROL

4.1. EFFECTS OF WING THICKNESS ON PERFORMANCE

Figure 17, based on data from Ref. 5, indicates that the XV-15 has a limiting Mach Number (M_{Mo}) of 0.575. This limit is due to compressibility-induced changes in steady or unsteady force or moment characteristics of the 23% thick airfoil. The corresponding Mach limit for the joined wing configuration of Fig. 13, which has NACA 64A212 airfoils, is estimated by comparing the Critical Mach Number, M_{crit}, for 12% and 23% thick 64-series airfoils. The Critical Mach Number is defined as the Mach Number at which local flow on the airfoil becomes supersonic. M_{Mo} for the joined wing configuration is estimated by assuming that the increase in M_{Mo} due to thinning the airfoil is equal to the increase in M_{crit}. Abbott, von Doenhoeff, and Stivers (Ref. 13) present airfoil data indicating that reducing the airfoil thickness from 23% to 12% at fixed C_L increases M_{crit} by 0.115. Hence the predicted limiting Mach number is 0.69. By using a more modern 12% thick airfoil, the limiting Mach Number could be increased to 0.75, provided the tail surfaces and propulsion system were capable of operating effectively at this higher Mach Number. At an altitude of 20,000 feet, the change in maximum Mach Number from 0.575 to 0.69 represents an increase in potential maximum speed of 70.7 knots. Using the advanced 12% airfoil, the potential speed gain is 107.5 knots.

As shown on Fig. 17, the XV-15 has a limiting speed of 300 knots EAS. This limit maintains adequate flutter margins. As shown in Ref. 8, the whirl flutter speed is not a function of EAS alone, because of the rotor dynamics; however, for trimmed level flight the deviation of flutter speed from constant EAS is not large. At low altitude, the 300-knot limit falls below the Mach limit of 0.575. At higher cruise altitudes the beneficial effect of increased cruise Mach Number can be utilized, even if the

flutter EAS boundary is not changed. As altitude increases, the Mach Number for a constant EAS also rises. For the XV-15, the 300 KEAS flutter boundary intersects the 0.575 Mach Number boundary at an altitude of 12,000 feet. Above this altitude the aircraft is Mach-limited rather than flutter-limited. A joined-wing tiltrotor having the same flutter boundary as the XV-15 would be able to fly at 300 KEAS at all altitudes up to 23,000 feet, above which it would be Mach-limited to 0.69. At 20,000 feet, the ceiling of the current XV-15, this represents a 70 knot difference in potential cruise speed with no change in flutter boundary.

The relative drag of the joined and cantilever wings at Mach numbers below that for drag divergence depends on the airfoil parasite drag coefficients and the span-efficiency factors of each wing set. At 6 million Reynolds number the minimum drag coefficient of the 12% 64A212 airfoil in a fully-turbulent condition is 0.009 while the minimum drag coefficient of the 23%-thick airfoil used on the cantilever XV-15 is 0.012 (Ref. 13). This 25% reduction in wing parasite drag is slightly offset by the reduction in wing Reynolds Number. The Reynolds Number of the XV-15 wing flying at 15,000 feet at 250 knots is 9.7 million. For the joined-wing configuration, the front-wing and rear-wing Reynolds Numbers are 6.5 million and 3.25 million respectively. Data in Ref. 13 show that the drag of the 64A212 airfoil is insensitive to Reynolds Number for Reynolds Numbers of 6 million and above. Thus, the front wing of the joined wing will enjoy the full parasite drag advantage of the thinner airfoil. At 3 million Reynolds Number, the parasite drag of the airfoil has risen 10% from its value at 6 million. Thus, the rear wing of the joined wing will have a $C_{d_{min}}$ of 0.0099. The area-weighted equivalent $C_{d_{min}}$ of the joined wing set is 0.0093, which is 22.5% less than the 0.012 of the cantilever 23% thick XV-15 wing at the same flight condition.

The performance of the joined-wing tiltrotor is also improved by the lower induced drag of the tip-jointed wing array. For the configuration of Fig. 13 the span efficiency of the joined wing is approximately 5% higher than that of the cantilever wing it replaces (Ref. 1). At the flight condition specified above, the cantilever-winged vehicle has an induced drag coefficient of 0.0204 while the joined-wing vehicle has an induced drag coefficient of 0.01945. The total wing parasite-plus-induced drag coefficient of the baseline, cantilever vehicle is 0.03240 while the joined-wing aircraft has a total wing-drag coefficient of 0.02875, which is 11.26% lower than that of the cantilever wing.

4.2 STABILITY AND CONTROL

The joined-wing configurations studied here retain the tail and vertical fins of the baseline XV-15. The joined wing array has an aerodynamic center which is 7.5 inches further aft of the front-wing leading-edge intersection with the fuselage than that of the cantilever wing. Accordingly, if the center of gravity is not moved, the joined-wing aircraft will have a higher static margin in airplane mode than the cantilever aircraft. The airplane-mode aft center-of-gravity limit of the XV-15 at the design gross weight of 13000 pounds is at FS 298 while the helicopter mode aft limit is at FS 301. With the joined wing, the airplane-mode aft center-of-gravity limit would move aft to FS 305, allowing the aircraft to use the aft portion of the baseline XV-15 helicopter-mode center-of-gravity envelope in all flight conditions. The airplane-mode forward center-of-gravity limit on the XV-15 is at FS 288.5 while the helicopter-mode forward limit is at FS 291.5. With the joined wing, the forward limit would move aft to FS 295.5. Thus, the allowable center-of gravity travel for the joined-wing aircraft using only the XV-15 horizontal tail for trim would be 5.5 inches as compared with 6.5 inches for the baseline XV-15. By using flaps on the joined

wings to aid in trimming the airplane, the forward center-of-gravity limit could be moved forward enough to give the joined-wing aircraft an allowable center-of-gravity travel the same as or greater than that of the baseline aircraft.

The front wing of Configuration 166-AL retains the leading-edge sweep and dihedral of the baseline cantilever wing. The rear wing is swept forward 15 degrees and has 23 degrees of dihedral. Accordingly, the joined-wing configuration is expected to have more stable dihedral effect than the cantilever baseline airplane.

4.3. CONFIGURATION INTEGRATION

Cross-Shafting: The passage of the current XV-15 cross-shaft through the 12% thick joined-wing front wing structure is shown in Fig. 18. There is ample clearance for the existing XV-15 shaft.

Fuel Volume: Reducing the thickness-to-chord ratio of the wing by 50% and separating the single, cantilevered, wing into a pair of joined wings reduces the total volume available within the wings for fuel. The joined-wing configuration has sufficient volume in the wings to carry 1,387 pounds of JP-4 fuel. This is 6.9% less than the maximum fuel capacity of the baseline XV-15 aircraft. Fuel is carried in both wings of the joined-wing vehicle.

5.0 AEROELASTIC CHARACTERISTICS

5.1 PROCEDURE FOR CALCULATING FLUTTER SPEEDS

Flutter speeds were calculated by a two-stage procedure. First, the mode shapes and frequencies (with no aerodynamic forces) were computed by the MSC-PAL program, as described in Section 1. Second, the mode shapes and frequencies of the lowest-frequency structural modes were input to CAMRAD. Three symmetric modes and three antisymmetric modes were selected. CAMRAD requires the mode shapes measured at the rotor hubs only, plus the generalized mass and the frequency of each mode. The remaining input data to CAMRAD was unchanged from that used for the baseline XV-15.

5.2 MODE SHAPES AND FREQUENCIES AT ZERO AIRSPEED

Table 4 summarizes the major configurations for which structural dynamic characteristics at zero airspeed were calculated. Tables 5 through 15 present the computed mode shapes and frequencies. Much can be learned from these Tables to supplement the flutter analyses presented later. The following points regarding the format of the Tables should be noted.

Mode Numbers: These typically go from 7 to 12, in order of increasing frequency. (Modes 1-6 are rigid-body modes, and are not required as input to CAMRAD.) In a few Tables some of modes 7 through 12 are replaced by higher-numbered modes. This is done to ensure that the three lowest-frequency symmetric modes and the three lowest-frequency antisymmetric modes are shown.

Hub Motions: The components of displacement and rotation at the starboard hub are presented, plus the root-sum-square (RSS) displacement and rotation, denoted as R for linear displacements

and ANGLE for angular displacements. The RSS quantities are used to normalize the linear and angular components. The normalized values of the components indicate which degree of freedom is dominant (e.g. a mode having Z/R =1 and X rotation/ANGLE = 1 is a pure beam bending mode). The relative magnitude of angular to linear motion is expressed by ANGLE/R. The ratio of Y rotation to Z displacement is also of interest, this is tabulated as PITCH/FLAP.

Modal Mass: Each modal mass is a term in the diagonal generalized mass matrix, which is equal to $[\phi]^T[m][\phi]$, where [m] is the nondiagonal mass matrix of the n-degree-of-freedom finite element model and $[\phi]$ is the [n x 1] vector representing the shape of the appropriate mode. The modal mass is given in units of slugs/12.

5.3 EFFECT OF GEOMETRY AND MASS DISTRIBUTION ON MODE SHAPES

Table 5 shows the baseline XV-15 model denoted as CAN-4L. The notation stands for cantilever wing, 4 elements per side in the finite-element model, light weight (=13,000 lb). The modes of greatest interest are the lowest frequency symmetric mode at 3.23 Hz, and the antisymmetric mode at 6.47 Hz. The flutter analysis (described later) shows that these are the modes that become unstable at the lowest speeds. Note that the pitch/flap ratio for the first symmetric mode is only 0.00254 rad/in. This is a low value which helps to keep the whirl flutter mode stable.

Table 6 shows the corresponding modal data for the baseline joined wing configuration shown in Fig. 13, denoted 166-AL. This also weighs 13,000 lb, but the nacelle mass distribution has been modified to represent a fixed-engine tilting rotor shaft configuration of the general type illustrated in Fig. 4. Relative to the cantilever configuration, the frequency of the

first symmetric mode has increased, but the pitch/flap ratio has increased by a factor of 4, and as will be described, this reduces the flutter speed.

The remaining Tables relate to variations in wing geometry and nacelle mass distribution that were investigated to determine their effects on flutter speed. These are discussed later in the present Section.

5.4 VALIDATION OF FLUTTER SPEED CALCULATIONS

The structural dynamic models employed to compute the mode shapes were simple, with only four spanwise elements per wing half. The fuselage and tail were represented by a uniform beam, as shown in Fig. 11. To check the accuracy of such a simple model for flutter calculations, its predictions were compared versus a more complete NASTRAN model used in previous studies (Ref. 14). Structural damping was set at 2% of critical damping. The MSC-PAL results agreed closely with the NASTRAN predictions of mode frequencies and flutter speeds, as shown in Figures 19, 20, 21, 22, and below.

FLUTTER SPEEDS PREDICTED BY NASTRAN AND MSC-PAL

MODE OF INSTABILITY:	1st SYMMETRIC	1st ANTISYMMETRIC
NASTRAN PLUS CAMRAD:	332 KEAS	337 KEAS
MSC-PAL PLUS CAMRAD (CASE CAN-4L)	335 KEAS	335 KEAS

The good agreement of the MSC-PAL flutter speeds with those computed by the more complex NASTRAN model is due to the close matching of the frequencies for the first three symmetric modes and the first two antisymmetric modes. MSC-PAL predicts too high a frequency for the antisymmetric torsion mode, but this mode goes unstable at a higher speed than the other modes, and so it is not a primary limit on aircraft speed. As the mode

frequencies increase and the mode shapes become more complex, the accuracy of a simple model such as the MSC-PAL model used here must necessarily become inferior to more detailed models. Thus a simple model might not suffice for vibration calculations. However, since it gives accurate predictions for flutter speeds of cantilever tiltrotors, it was employed to calculate joined-wing flutter speeds as described below.

5.5 FLUTTER CHARACTERISTICS OF JOINED-WING TILTROTORS

EFFECT OF NACELLE C.G. POSITION: Figure 13 shows the starting point for our studies of joined wing tiltrotors. The configuration of Fig. 13 was assigned the number 166; code letters AL, BL, CL, were attached to denote different nacelle mass distributions, with the nacelle mass and the gross weight (13,000 lb) held constant. The CL nacelle models the current XV-15. The c.g. of the BL nacelle is approximately 2 inches aft of the c.g of the current XV-15 nacelle. The AL nacelle c.g. is approximately 7 inches aft of the XV-15 nacelle c.g. Thus 166-AL, 166-BL, 166-CL all represent joined-wing tiltrotors with 12% thick wings, with sweep angles of -6.5 degrees (front) and -15 degrees (rear).

The effect of nacelle mass distribution on flutter speed is relatively small, as shown in Fig. 23. All the variants have flutter speeds in the 240-245 KEAS region. This is less than the cantilever value of 335 KEAS. To trace the reason for the lower flutter speed, the first symmetric and antisymmetric mode characteristics were examined. From Tables 5, 6, 7, 8, denoting the pitch/flap ratio in rad/in as P/F:

MODE:	1st Symmetric				1st Antisymmetric			
CASE:	CAN-4L	166-AL	166-BL	166-CL	CAN-4L	166-AL	166-BL	166-CL
FR,Hz.	3.24	4.17	4.07	3.65	6.47	4.26	3.94	4.75
P/F	0.0025	0.0106	0.0120	0.0114	0.0291	0.0143	0.0134	0.0206

Considering first the symmetric mode, the above comparison shows that although the joined wing can increase the mode frequency by 29%, the pitch/flap ratio also goes up by a factor of 4.2. For the antisymmetric mode the pitch/flap ratio is halved, but the frequency is reduced to 61% of the cantilever value.

To check the importance of the pitch motion as the cause of the reduced flutter speed, a joined wing case similar to 166-AL was re-run with the hub pitch motion arbitrarily set to zero. This raised the flutter speed to 285 KEAS for the 1st symmetric mode and 430 KEAS for the first antisymmetric mode. This result suggested that higher flutter speeds could be obtained by modifying the geometry and mass distribution of the joined wings such that the pitch/flap ratio would be reduced, provided this could be done without lowering the frequencies of the first symmetric and antisymmetric modes. The configuration variations described below were aimed at achieving these modal characteristics.

EFFECT OF WING THICKNESS: The thickness/ chord ratio of the front wing was increased to 15%, leaving the rear wing unchanged at 12%. The wings were re-stressed, and mode characteristics and flutter characteristics calculated (see Tables 9, 10, and 11). The thicker wing cases are designated 266-AL, 266-BL, and 266-CL, retaining the previous notation for nacelle c.g. position. The results are graphed in Figs. 24 and 25. As shown in Fig. 24, increasing the front wing thickness by 3% raises the symmetric mode flutter speed to 260 KEAS. The antisymmetric mode shows a larger increase, reaching 295 KEAS if the current nacelle

location is retained. It is expected that a further increase would be obtained if the rear wing thickness were also increased.

It is instructive to compare the mode shapes of the first symmetric modes for Cases 266-CL and 166-CL versus the baseline cantilever case, as follows.

CASE	FREQUENCY, Hz	PITCH/FLAP, rad/in	FLUTTER SPEED, KEAS
CAN-4L	3.24	0.00254	335 Symmetric
266-CL	4.02	0.01021	260 " "
166-CL	4.17	0.01060	245 " "

The above comparison supports the previous indication that reducing the hub pitch motion may be more beneficial than increasing the mode frequency. On this basis it was decided to to investigate planform variations instead of further increases in wing thickness.

EFFECT OF WING SWEEP: The front wing of the 166 and 266 series configurations shown in Fig. 13 has -6.5 degrees sweep. This is the same as the XV-15 wing, and the rotor clearance is identical. Alternative configurations with positive sweep on the front wing were investigated; these require nacelle modifications to maintain the same rotor clearance, as discussed later.

Tables 12, 13, and 14 present mode shapes for four configurations with positive sweep (i.e. sweepback) on the front wing. The configurations are denoted as 467-AL, 468-AL, and 467-DH. All have the same rear wing sweep as the baseline joined wing, i.e. -15 degrees. The 467 configurations have 6.5 degrees sweepback, and the 468 configurations have 15 degrees sweepback on the front wing. The wing tips are in the same location as the 166 and 266 wings, so the root of the front wing is located further forward on the fuselage than the location shown in Fig. 13. The -AL nacelle was retained for most of the cases studied,

but the effect of a longer mast was explored in Configuration 467-DH. This has rotor hubs moved 44 inches forward of the XV-15 position, to obtain the same clearance between the rotor and the wing root as on the XV-15. The extra drive shaft length, supporting structure, and nacelle extension is assumed to weigh 200 lb per nacelle, increasing the gross weight from 13,000 lb to 13,400 lb. The notation 467-DH denotes the modified nacelle (type D) and the heavier gross weight.

Increasing sweepback reduces the pitch/flap ratio, as indicated below.

MODE:	1st Symmetric			1st Antisymmetric		
SWEEP:	-6.5°	6.5°	15°	-6.5°	6.5°	15°
CASE:	CAN-4L	467-AL	468-AL	CAN-4L	467-AL	468-AL
FR,Hz.	3.24	3.62	3.19	6.47	4.24	4.26
P/F	0.0025	0.0033	-0.0008	0.0291	0.0145	0.0146

On this basis one would expect that the flutter speed of the first symmetric mode of the 15-degree sweep configuration would match that of the baseline cantilever case (335 KEAS). However, as shown on Fig. 26, the flutter speed only increases to 260 KEAS (from 245 KEAS for the -6.5 degree sweep joined wing). For the first antisymmetric mode the improvement is also small (Fig. 27). The explanation appears to be that the yaw and fore and aft components of the hub motion have both been increased by sweep, and couple adversely with the rotor dynamics, so that the whirl mode now involves fore-and-aft linear hub motion in addition to vertical displacement.

6.0 POSSIBLE DEVELOPMENT DIRECTIONS

6.1 DISCUSSION OF FINDINGS OF CURRENT STUDY

The work completed in Phase 1 of this effort has shown that a joined-wing tiltrotor vehicle can be built which will have wings of half of the thickness/chord ratio of current cantilever-wing tiltrotors. This reduction in wing t/c potentially increases the limiting Mach Number of the aircraft, thus increasing aerodynamic speed potential by over 100 knots.

The flutter boundary of the baseline joined-wing tiltrotor configuration shown in Fig. 13 is not high enough to exploit this increased Mach Number potential at low altitude. Thus, the aircraft is limited by flutter over most of its altitude range. This can be addressed in two different ways.

For the baseline joined-wing tiltrotor the flutter boundary was defined with the proprotors running, propelling the aircraft. If the rotors were stopped and folded in flight, the aircraft would have a higher critical flutter speed with the rotors folded than with them turning. A second, high-speed propulsion system could then drive the aircraft to speeds limited primarily by the Mach Number characteristics of the wing.

Another approach is to increase the critical flutter speed of the vehicle with the rotors turning. One way to do this is to increase the thickness of the wing. Increasing wing thickness will increase the flutter speed and decrease the Mach Numbers at which drag divergence and buffet set in. The baseline joined-wing tiltrotor is not a balanced design because the flutter speed is significantly lower than the limiting Mach Number. A balanced design would have the Mach Number and flutter boundaries at or near the same airspeed for a typical cruise condition. These

boundaries would be higher than for the cantilever vehicle. This approach would offer a near-term way to increase tiltrotor cruise speed.

The possible performance improvements defined in the current Phase 1 study indicate many ways to improve the performance of future tiltrotor aircraft, as listed below. Appropriate study tasks in each category are denoted by asterisked paragraphs.

6.2 CONFIGURATION AND OPERATIONAL CONCEPTS.

6.2.1. NON-FOLDING TILTROTORS

6.2.1.1. Medium Speed Vehicle with flight envelope similar to current tiltrotors (Maximum Speed: 300 KEAS).

* Delineate effects of structural configuration on mode shapes. Define a parametric matrix of configurations with variations in sweep, thickness, dihedral, and nacelle length, planform and material distribution. For each configuration design the structure for static loading. Calculate mode shapes and frequencies, and determine trends and sensitivities.

* Study effects of mode shapes on flutter. Using results from the task above, determine the flutter characteristics of each configuration. Analyze the results and isolate mode-shape effects on flutter speed.

6.2.1.2. High Speed Vehicle (400-450 KEAS).

* Analyze as 6.2.1.1., including Mach Number effects.

6.2.2. FOLDING TILTROTORS

6.2.2.1. High-Speed Subsonic Aircraft.

6.2.2.2. Transonic Aircraft.

6.2.3. TILTPROPFANS

6.2.3.1 The Tiltpropfan (Fig. 28) is a new class of VTOL aircraft that falls between tiltrotors and jet-lift aircraft in disk loading. In addition to VTOL, the aircraft would be capable of airplane-mode takeoff and landing, and flight at high subsonic Mach Numbers.

* Study utility and feasibility of this new class of VTOL aircraft.

6.3 AEROELASTICITY

6.3.1 EFFECT OF INCREASING WING STIFFNESS

6.3.1.1 Composite Materials.

* Perform design studies of composite-structured configurations. Design structures for static loading. Evaluate flutter characteristics, and compare with metal structures. Study effects of ply orientation to control relationship between wing flexure and torsion.

6.3.1.2. Increased thickness/chord: balanced configuration.

* Define a matrix of configurations with parametric variations in sweep and t/c. Design structures for static loading. Evaluate flutter characteristics, and determine trends and sensitivities.

6.3.2. ROTOR HUB REDESIGN

6.3.2.1. Pylon-Swashplate Coupling.

6.3.2.2. Delta-three and other hinge variations.

6.3.2.3. Rigid Rotors and Blade-Flapping Restraint

6.3.3. INNOVATIVE APPROACHES TO WING/ROTOR CLEARANCE

6.3.3.1. Use of automatic flight control to reduce flapping. This requires a highly redundant electromechanical system to ensure safety at all flight conditions. Blade flapping would be sensed and fed back to blade pitch controls.

6.3.4 STUDY OF JOINED WING/ROTOR DYNAMIC COUPLING PHENOMENA

* Develop theory to predict effect of mode shapes and frequencies on rotor stability. Develop methodology to design joined wings having desirable mode shapes. This methodology should guide the selection of sweep, dihedral, and thickness/chord ratio of front and rear wings. Design model experiments to verify the theory and methodology developed above. Build and test

models designed above. Compare test results with theory, and refine theory.

6.4. HOVER AERODYNAMICS

6.4.1 STUDY EFFECT OF JOINED WINGS ON HOVER DOWNLOAD

* Design experiment to study effect of various joined-wing configurations on hover download. Build and test model, develop predictive theory.

6.5. CRUISE AERODYNAMICS

6.5.1 STUDY EFFECT OF JOINED WINGS ON STABILITY AND CONTROL

* Study longitudinal and lateral-directional stability and control. Check results with wind-tunnel model.

6.5.2. STUDY EFFECTS OF JOINED-WING WEIGHT SAVINGS ON PERFORMANCE

*The weight savings of the joined wing can be traded for increased span and/or reduced hover and cruise power. Study these trade-offs to delineate optimum configurations.

7.0 CONCLUSIONS AND RECOMMENDATIONS

7.1 CONCLUSIONS

1. The application of the joined wing to tiltrotor aircraft would permit current cantilever wings with thickness/chord ratios of 23% to be replaced by joined wings of 12% thickness/chord ratio with less weight and drag having equal static strength.

2. Such thin joined wings would raise the limiting Mach Number by approximately 0.18 and increase maximum speed capability by over 100 knots.

3. The flutter boundary of a baseline joined wing configuration having 12% thick airfoils combined with the fuselage, tail, nacelles and rotors of the XV-15 was computed to be approximately 245 knots EAS. This is not high enough to exploit the increased Mach Number potential of the thin joined wings at low altitude. This limitation can be circumvented by employing rotors which can be stopped and folded in flight, below the critical flutter speed. A more general solution would be to modify the baseline airframe to raise its flutter speed.

4. Several modifications of the baseline joined-wing configuration were studied to examine their effect on flutter speed and to gain an understanding of the phenomena involved. These included increasing the thickness/chord ratio of the front wing to 15%, which increased the flutter speed to approximately 260 knots. A similar increase was obtained through adopting 15 degrees sweepback on the front wing. This introduces some problems of rotor/wing clearance which may require longer nacelles. The present study did not yield a joined wing configuration with desirable flutter speeds, however the scope of the study only permitted 9 configurations to be analyzed. There

does not appear to be any fundamental reason why such a configuration should not be found with further effort, after the joined wing/rotor coupling is more fully understood.

5. The flutter speed limitation was found to be caused by coupling of rotor dynamics with the first symmetric and first antisymmetric wing modes. For a cantilever wing these are essentially beam bending modes, primarily comprised of wing flapping and torsion. For the joined wing the modes are more complex, involving fore-and-aft and lateral motion of the rotor hubs. The rotor/wing coupling mechanism has not been identified sufficiently clearly to indicate the best solution. Possible approaches include increased thickness of both front and rear wings, increased wing stiffness through optimum material distribution, increased stiffness through the use of composites, and modifications of wing sweep, dihedral, and other geometric parameters to reduce the amplitudes of yawing and pitching at the hub in the first symmetric and antisymmetric wing bending modes.

7.2. RECOMMENDATIONS FOR FURTHER WORK

1. In planning further work the relative priority of stopped and folding versus conventional rotors should be determined. There do not appear to be any special barriers to application of the joined wing to stopped-rotor configurations, and the prospect of a 100-knot increase in speed capability is attractive. Some research should be done on stopped-rotor configurations, since the thin airfoils permitted by joined wings allow the vehicle to enter the speed regime where jet propulsion is efficient.

2. As regards conventional (non-stoppable) rotors, which propel the aircraft during cruise, the following recommendations are made.

3. A more complete understanding is required of how the motion of the joined wing couples with the blade dynamics. This understanding should be obtained through a linked program of basic theoretical studies, computer analyses of configuration variations, and wind-tunnel model tests.

4. It is desirable to simplify the problem by breaking it down into parts. One part would consider the joined wing as a separate unit and would investigate the effect of various geometric and mass distribution changes on the mode shapes and frequencies. Another part would focus on the effects of given mode shapes and frequencies on flutter speed for given rotor dynamics. A third part would consider the effects of changing the rotor dynamics through hinge design or innovative approaches such as toed-out rotors. By combining the results of these partial studies a feasible configuration would be derived. This configuration can then be wind-tunnel tested, and its hover download characteristics measured in a model test.

4. Section 6 of this report details the tasks and subtasks appropriate to the general research areas outlined above.

REFERENCES

1. Wolkovitch, J., The Joined Wing: An Overview, J. Aircraft, Vol. 23, No. 3, March 1986, p. 161-178.

2. Popelka, D., M. Sheffler, and J. Bilger, Correlation of Test and Analysis for the 1/5-Scale V-22 Aeroelastic Model, J. American Helicopter Society, April 1987, p.22-33.

3. Felker, F. F., and J. S. Light, Aerodynamic Interactions Between a Wing and a Rotor in Hover, J. American Helicopter Society, April 1988, p.53-61.

4. Johnson, W., B. H. Lau, and J. V. Bowles, Calculated Performance, Stability, and Maneuverability of High Speed Tilting Proprotor Aircraft, Vertica, Vol.11, No.1/2, 1987, p.317-339.

5. Maisel, M.D., Tilt Rotor Research Aircraft Familiarization Document, NASA TM X-62, 407, January 1975.

6. Staff of Bell Helicopter Co., Bell Helicopter V/STOL Tilt Rotor Research Aircraft Volume 3: Structural Loads and Dynamics, Bell Helicopter Co. Report No. 301-199-003, 1974.

7. Johnson, W., Assessment of Aerodynamic and Dynamic Models in A Comprehensive Analysis for Rotorcraft, Comp. & Maths. with Appls., Vol 12A, No. 1, 1986, p.11-28.

8. Johnson, W., An Assessment of the Capability to Calculate Tilting Prop-Rotor Aircraft Performance, Loads, and Stability, NASA TP 2291, March 1984.

9. Johnson, W., Development of a Comprehensive Analysis for Rotorcraft I. Rotor Model and Wake Analysis, Vertica, Vol.5, 1981, p99-129.

10. Johnson, W., Development of a Comprehensive Analysis for Rotorcraft II. Aircraft Model, Solution Procedure and Applications, Vertica, Vol.5, 1981, p185-216.

11. Acree, C.W., Jr., and M. B. Tischler, Identification of XV-15 Aeroelastic Modes Using Frequency Sweeps, J. Aircraft, Vol. 26, No. 7, July 1989, p667-674.

12. Foch, R.J., and R.E. Wyatt, Low Altitude/Airspeed Unmanned Research Aircraft (LAURA) Preliminary Development, Proc. International Conference on Aerodynamics at Low Reynolds Numbers, Royal Aeronautical Soc., London, October 1986, Vol III, p.31.1-31.29.

13. Abbott, I.H., A.E. von Doenhoff, and L. S. Stivers, Jr., Summary of Airfoil Data, NACA Report No. 824, 1945.

14. Schroers, L.G., Dynamic Structural Aeroelastic Stability Testing of the XV-15 Tilt Rotor Research Aircraft, NASA TM 84293, 1982.

TABLE 1. XV-15 WEIGHT BREAKDOWN

COMPONENT	WEIGHT LB.
WING	946
BLADES	590
HUB & HINGE	273
TAIL	259
BODY	1,589
LANDING GEAR	524
COWL	309
NACELLE (LESS COWL)	60
SPINNER	71
ENGINES	1,052
COUPLING GEARBOX	82
GEARBOXES & ROTOR DRV	1,205
DRIVE SHAFTS	53
PROPULSION SUBSYSTEMS	141
EXHAUST SYSTEM	10
FUEL TANKS	159
FUEL SYS. PLUMBING	67
COCKPIT CONTROLS	45
AFCS	165
ROTOR FC (NB)	262
ROTOR FC (BOOST)	190
ROTOR FC HYD. SYS.	177
CONVERSION SYS, & HYD.	273
FIXED WING FC & HYD	294
BASIC AIRFRAME	8,796
TOTAL AIRFRAME EQUIPMT	1,288
TOTAL MISSION EQUIPMT	1,148
TOTAL EMPTY WEIGHT	11,232
BALLAST	106
ENGINE OIL	53
ENGINE OIL TRAPPED	8
FUEL TRAPPED	88
USEABLE FUEL	1,111
CREW	380
MAG TAPE	12
FLIGHT BAG	10
T.O WEIGHT	13,000

TABLE 2. XV-15 MSC-PAL STRUCTURAL MODEL WITH 4 WING ELEMENTS

	density lbs./in	length L, in	dist. den.X L	conc. at X=236.18	conc. at X=341.18	total weight X 2
NACELLE	15.1	105	1585.5	558.73		4288.46
FUSELAGE	12.288	505	6205.44			6205.44
WING						
node1 - node2	1 - 2	2 - 3	3 - 4	4 - 5		
EIXX	3.7E+09	3.7E+09	3.7E+09	3.7E+09		
EIZZ	1.1E+10	1.1E+10	1.1E+10	1.1E+10		
length, in	48.25	48.25	48.25	48.25		
density, lb/in	2.17	5.97	8.69	9.26		
weight, lb.	104.7025	288.0525	419.2925	446.795		2517.685
TOTAL AIRPLANE WEIGHT						13011.58

TABLE 3. COMPARISON OF PREDICTED STRUCTURAL MODE FREQUENCIES FROM MSC-PAL, CAMRAD AND GROUND VIBRATION TESTS

Wing Bending Modes	Natural Frequency Hz		
	Measured (in flight Ref. 8)	Predicted by NASTRAN (1974)	Predicted by MSC-PAL
Symmetric beam bending	3.4	3.1	3.2
Asymmetric beam bending	6.3	6.7	6.7
Symmetric chord bending	6.6	6.3	5.2
Asymmetric chord bending	7.9	8.7	6.5
Symmetric torsional bending	8.2	8.2	7.2
Asymmetric torsional bending	7.7	7.5	27.9

* First NASTRAN model did not include a wing-fuselage shear tie member. Inclusion of this member increased stiffness and frequency.

TABLE 4. PRINCIPAL CONFIGURATIONS ANALYSED

All configurations retained the XV-15 tail, which has zero sweep and a thickness/chord ratio of 15%.

Gross Wt. = 13,000 lb, unless otherwise noted.

CASE	DESCRIPTION	THICKNESS %		SWEEP, deg	
		Front	Rear	Front	Rear
CAN-4L	Baseline XV-15 Nacelle c.g.at F.S.288.68 Wing weight = 946 lb.	23	--	-6.5	--
166-AL	Joined Wing: Nacelle c.g.at F.S.281.88 Wing weight = 858 lb.	12	12	-6.5	-15
166-BL	Joined Wing: Nacelle c.g.at F.S.286.88 Wing weight = 858 lb.	12	12	-6.5	-15
166-CL	Joined Wing: Nacelle c.g.at F.S.288.68 Wing weight = 858 lb	12	12	-6.5	-15
266-AL	Joined Wing: Nacelle c.g.at F.S.281.88 Wing weight = 867 lb.	15	12	-6.5	-15
266-CL	Joined Wing: Nacelle c.g.at F.S.288.68 Wing weight = 867 lb.	15	12	-6.5	-15
467-AL	Joined Wing: Nacelle c.g.at F.S.281.88 Wing weight = 840 lb.	12	12	+6.5	-15
467-DH	Joined Wing: 13,400 lb. Hubs moved forward 44in. Nacelle c.g.at F.S.259.80 Wing weight = 840 lb.	12	12	+6.5	-15
468-AL	Joined Wing: Nacelle c.g.at F.S.281.88 Wing weight = 877 lb.	12	12	+15	-15

TABLE 5. MODE SHAPES AT STARBOARD HUB FOR XV-15 (CASE: CAN-4L)

CASE	CAN-4L					
MODE No.	7	8	9	10	11	16
FREQUENCY, Hz.	3.23724	5.19072	6.47859	6.72807	7.14498	27.939
SYM. OR ASYM.	S	S	A	A	S	A
STARBOARD HUB						
X, in	-0.0000	0.31484	-0.2588	0.00000	-0.0000	-0.0000
Y, in	0.00000	0.28379	-0.1712	0.00000	-0.0000	0.00000
Z, in	-0.4000	0.00000	0.00000	0.37157	-0.3201	-0.3384
R=SR(X^2+Y^2+Z^2)	0.40002	0.42386	0.31037	0.37157	0.32014	0.33842
X/R	-0.0000	0.74278	-0.8339	0.00000	-0.0000	-0.0000
Y/R	0.00000	0.66953	-0.5518	0.00000	-0.0000	0.00000
Z/R	-1	0.00000	0.00000	1	-1	-1
X ROT., rad	-0.0043	0.00000	-0.0000	-0.0010	0.00199	0.00006
Y ROT., rad	-0.0010	-0.0000	0.00000	0.00902	-0.0087	-0.0088
Z ROT., rad	-1E-10	-0.0041	0.00312	-0.0000	0.00000	-0.0000
ANGLE = MOD(ROT)	0.00443	0.00410	0.00312	0.00908	0.00896	0.00885
X ROT / ANGLE	-0.9731	0.00000	-0.0000	-0.1103	0.22292	0.00720
Y ROT / ANGLE	-0.2300	-0.0000	0.00000	0.99389	-0.9748	-0.9999
Z ROT / ANGLE	-0.0000	-1	1	-0.0000	0.00000	-0.0000
ANGLE/R, rad/in	0.01107	0.00967	0.01007	0.02444	0.02801	0.02617
PITCH/FLAP, rd/in	0.00254	-0.2386	0.02905	0.02430	0.02730	0.02617
MODAL MASS slg/12	2.472	2.258	2.186	1.332	1.29	1.666
MM * FREQ.SQR	25.9058	60.8385	91.7510	60.2955	65.8554	1300.45

Note: In this and subsequent Tables the pitch/flap ratio is equal to Y ROT/ Z radians per inch.

TABLE 6. MODE SHAPES AT STARBOARD HUB FOR JOINED WING #166-AL

CASE	166 AL					
MODE No.	7	8	9	10	11	12
FREQUENCY, Hz.	4.17262	4.26186	4.73573	6.90927	7.02643	8.23203
SYM. OR ASYM.	S	A	S	A	S	A
STARBOARD HUB						
X, in	-0.0721	0.00023	0.15906	0.02334	-0.0050	-0.1666
Y, in	-0.0713	-0.0080	0.1679	0.01557	-0.0052	-0.1968
Z, in	-0.5239	0.50599	-0.2028	-0.0322	0.03673	-0.0336
R=SR(X^2+Y^2+Z^2)	0.53373	0.50605	0.30764	0.04277	0.03745	0.26015
X/R	-0.1351	0.00045	0.51703	0.54587	-0.1358	-0.6407
Y/R	-0.1337	-0.0159	0.54576	0.36406	-0.1401	-0.7567
Z/R	-0.9817	0.99987	-0.6594	-0.7546	0.98076	-0.1295
X ROT., rad	-0.0029	0.00156	0.00099	0.00187	-0.0015	-0.0011
Y ROT., rad	-0.0055	0.00725	-0.0050	-0.0009	0.00085	-0.0005
Z ROT., rad	0.00106	0.00025	-0.0025	-0.0003	0.00008	0.00243
ANGLE = MOD(ROT)	0.00639	0.00742	0.00572	0.00212	0.00173	0.00273
X ROT / ANGLE	-0.4662	0.21117	0.17355	0.88295	-0.8690	-0.4151
Y ROT / ANGLE	-0.8688	0.97683	-0.8744	-0.4360	0.49246	-0.1903
Z ROT / ANGLE	0.16632	0.03459	-0.4530	-0.1739	0.04773	0.88959
ANGLE/R, rad/in	0.01197	0.01467	0.01859	0.04957	0.04639	0.01052
PITCH/FLAP, rd/in	0.01060	0.01434	0.02465	0.02864	0.02329	0.01546
MODAL MASS,slg/12	1.417	1.301	1.664	0.3492	0.3371	1.317
MM * FREQ.SQR	24.6710	23.6306	37.3187	16.6701	16.6428	89.2482

TABLE 7. MODE SHAPES AT STARBOARD HUB FOR JOINED WING #166-BL

CASE	166 BL					
MODE No.	7	8	9	10	11	12
FREQUENCY, Hz.	3.9424	4.07218	4.49656	6.84807	6.98439	8.18358
SYM. OR ASYM.	A	S	S	A	S	A
STARBOARD HUB						
X, in	-0.0013	-0.0153	0.18059	0.02270	0.00165	-0.1623
Y, in	0.01209	-0.0124	0.18853	0.01675	0.00152	-0.2013
Z, in	-0.5354	-0.5513	0.06500	-0.0127	-0.0207	-0.0284
R=SR(X^2+Y^2+Z^2)	0.53562	0.55174	0.26903	0.03094	0.02088	0.26022
X/R	-0.0026	-0.0277	0.67124	0.73368	0.07914	-0.6239
Y/R	0.02257	-0.0225	0.70075	0.54145	0.07297	-0.7737
Z/R	-0.9997	-0.9993	0.24160	-0.4105	-0.9941	-0.1092
X ROT., rad	-0.0015	-0.0022	0.00241	0.00189	0.00151	-0.0010
Y ROT., rad	-0.0071	-0.0066	-0.0019	-0.0005	-0.0005	-0.0004
Z ROT., rad	-0.0002	0.00015	-0.0028	-0.0003	-0.0000	0.00243
ANGLE = MOD(ROT)	0.00735	0.00700	0.00422	0.00201	0.00162	0.00270
X ROT / ANGLE	-0.2135	-0.3255	0.57159	0.93951	0.93295	-0.4009
Y ROT / ANGLE	-0.9763	-0.9452	-0.4497	-0.2917	-0.3596	-0.1633
Z ROT / ANGLE	-0.0352	0.02145	-0.6862	-0.1793	-0.0166	0.90143
ANGLE/R, rad/in	0.01373	0.01270	0.01570	0.06502	0.07759	0.01038
PITCH/FLAP, rd/in	0.01340	0.01201	-0.0292	0.04621	0.02806	0.01552
MODAL MASS,slg/12	1.47	1.457	1.834	0.3415	0.3307	1.304
MM * FREQ.SQR	22.8475	24.1609	37.0817	16.0150	16.1321	87.3301

TABLE 8. MODE SHAPES AT STARBOARD HUB FOR JOINED WING #166-CL

CASE	166 CL					
MODE No.	7	8	9	10	11	12
FREQUENCY, Hz.	3.65416	4.75271	5.55706	7.29487	7.42252	8.13164
SYM. OR ASYM.	S	A	S	S	A	A
STARBOARD HUB						
X, in	0.07347	0.00251	-0.1265	-0.0341	-0.0324	-0.1576
Y, in	0.07707	-0.0089	-0.1318	-0.0340	-0.0104	-0.1706
Z, in	0.45298	-0.2578	0.14387	0.06546	0.08412	-0.0339
R=SR(X^2+Y^2+Z^2)	0.46532	0.25805	0.23253	0.08129	0.09076	0.23478
X/R	0.15789	0.00976	-0.5440	-0.4197	-0.3575	-0.6715
Y/R	0.16564	-0.0345	-0.5667	-0.4188	-0.1153	-0.7267
Z/R	0.97346	-0.9993	0.61869	0.80520	0.92676	-0.1448
X ROT., rad	0.00313	-0.0011	0.00001	-0.0015	-0.0017	-0.0010
Y ROT., rad	0.00515	-0.0053	0.00400	0.00178	0.00253	-0.0006
Z ROT., rad	-0.0011	-0.0001	0.00199	0.00049	0.00048	0.00235
ANGLE = MOD(ROT)	0.00614	0.00545	0.00447	0.00241	0.00312	0.00267
X ROT / ANGLE	0.51027	-0.2182	0.00380	-0.6410	-0.5623	-0.3994
Y ROT / ANGLE	0.83910	-0.9755	0.89534	0.73952	0.81232	-0.2562
Z ROT / ANGLE	-0.1884	-0.0268	0.44534	0.20535	0.15459	0.88021
ANGLE/R, rad/in	0.01320	0.02113	0.01923	0.02970	0.03438	0.01138
PITCH/FLAP, rd/in	0.01138	0.02063	0.02783	0.02728	0.03013	0.02015
MODAL MASS,Slg/12	1.833	0.6387	0.8316	0.3747	0.3931	1.295
MM * FREQ.SQR	24.4758	14.4271	25.6805	19.9397	21.6573	85.6300

TABLE 9. MODE SHAPES AT STARBOARD HUB FOR JOINED WING #266-AL

CASE No.	266 AL					
MODE No.	7	8	9	10	11	12
FREQUENCY, Hz.	4.53259	4.89449	5.1621	7.08601	7.18574	8.45909
SYM. OR ASYM.	S	A	S	A	S	A
STARBOARD HUB						
X, in	0.13292	0.00058	-0.1031	0.02176	0.00628	-0.1717
Y, in	0.13594	-0.0074	-0.1099	0.01333	0.00608	-0.2005
Z, in	0.41547	0.48477	0.38417	-0.0444	-0.0475	-0.0360
R=SR(X^2+Y^2+Z^2)	0.45690	0.48482	0.41267	0.05124	0.04834	0.26643
X/R	0.29091	0.00120	-0.2499	0.42467	0.13010	-0.6445
Y/R	0.29752	-0.0154	-0.2663	0.26018	0.12580	-0.7525
Z/R	0.90931	0.99987	0.93092	-0.8671	-0.9834	-0.1351
X ROT., rad	0.00312	0.00132	0.00024	0.00122	0.00089	-0.0012
Y ROT., rad	0.00323	0.00693	0.00641	-0.0010	-0.0009	-0.0005
Z ROT., rad	-0.0020	0.00023	0.00170	-0.0003	-0.0000	0.00248
ANGLE = MOD(ROT)	0.00494	0.00706	0.00664	0.00165	0.00133	0.00285
X ROT / ANGLE	0.63071	0.18755	0.03623	0.73845	0.67341	-0.4532
Y ROT / ANGLE	0.65448	0.98170	0.96583	-0.6427	-0.7359	-0.1894
Z ROT / ANGLE	-0.4169	0.03292	0.25662	-0.2039	-0.0702	0.87099
ANGLE/R, rad/in	0.01082	0.01457	0.01610	0.03234	0.02763	0.01070
PITCH/FLAP, rd/in	0.00779	0.01430	0.01670	0.02397	0.02067	0.01501
MODAL MASS slg/12	1.558	1.215	1.405	0.3465	0.3361	1.370
MM * FREQ.SQR	32.0081	29.1065	37.4394	17.3982	17.3544	98.0319

TABLE 10. MODE SHAPES AT STARBOARD HUB FOR JOINED WING #266-BL

CASE	266 BL					
MODE No.	7	8	9	10	11	12
FREQUENCY, Hz.	4.53093	4.56145	4.7488	7.00945	7.13072	8.40164
SYM. OR ASYM.	A	S	S	A	S	A
STARBOARD HUB						
X, in	-0.0013	0.13145	-0.1058	0.02099	0.00199	-0.1674
Y, in	0.01170	0.13462	-0.1123	0.01435	0.00152	-0.2051
Z, in	-0.5522	0.42555	0.39102	-0.0203	-0.0275	-0.0305
R=SR(X^2+Y^2+Z^2)	0.55240	0.46528	0.42039	0.03256	0.02770	0.26654
X/R	-0.0023	0.28251	-0.2518	0.64468	0.07207	-0.6282
Y/R	0.02119	0.28932	-0.2672	0.44082	0.05489	-0.7695
Z/R	-0.9997	0.91459	0.93013	-0.6245	-0.9958	-0.1145
X ROT., rad	-0.0013	0.00308	0.00006	0.00125	0.00091	-0.0012
Y ROT., rad	-0.0070	0.00331	0.00642	-0.0006	-0.0006	-0.0004
Z ROT., rad	-0.0002	-0.0020	0.00175	-0.0003	-0.0000	0.00248
ANGLE = MOD(ROT)	0.00717	0.00496	0.00666	0.00145	0.00112	0.00282
X ROT / ANGLE	-0.1901	0.62144	0.00997	0.86347	0.81482	-0.4434
Y ROT / ANGLE	-0.9811	0.66677	0.96461	-0.4518	-0.5792	-0.1613
Z ROT / ANGLE	-0.0343	-0.4113	0.26346	-0.2241	-0.0229	0.88164
ANGLE/R, rad/in	0.01298	0.01067	0.01584	0.04470	0.04049	0.01058
PITCH/FLAP, rd/in	0.01274	0.00778	0.01643	0.03234	0.02355	0.01491
MODAL MASS,Slg/12	1.424	1.526	1.678	0.3353	0.3269	1.359
MM * FREQ.SQR	29.2337	31.7512	37.8407	16.4740	16.6219	95.9284

TABLE 11. MODE SHAPES AT STARBOARD HUB FOR JOINED WING #266-CL

CASE	266 CL					
MODE No.	7	8	9	10	11	12
FREQUENCY, Hz.	4.01614	5.39514	5.93501	7.49512	7.69044	8.35575
SYM. OR ASYM.	S	A	S	S	A	A
STARBOARD HUB						
X, in	-0.0981	-0.0001	0.10876	-0.0402	-0.0313	0.16379
Y, in	-0.1035	0.00866	0.11252	-0.0395	-0.0071	0.17492
Z, in	-0.4293	0.23108	-0.1574	0.08162	0.10695	0.03560
R=SR(X^2+Y^2+Z^2)	0.45242	0.23124	0.22200	0.09922	0.11167	0.24226
X/R	-0.2169	-0.0006	0.48989	-0.4055	-0.2804	0.67608
Y/R	-0.2289	0.03745	0.50683	-0.3984	-0.0643	0.72202
Z/R	-0.9489	0.99929	-0.7093	0.82264	0.95770	0.14695
X ROT., rad	-0.0030	0.00092	-0.0000	-0.0009	-0.0011	0.00124
Y ROT., rad	-0.0043	0.00470	-0.0038	0.00206	0.00297	0.00068
Z ROT., rad	0.00156	0.00009	-0.0016	0.00057	0.00045	-0.0024
ANGLE = MOD(ROT)	0.00558	0.00479	0.00420	0.00235	0.00322	0.00280
X ROT / ANGLE	-0.5530	0.19274	-0.0032	-0.4154	-0.3587	0.44300
Y ROT / ANGLE	-0.7845	0.98104	-0.9156	0.87671	0.92271	0.24547
Z ROT / ANGLE	0.28043	0.01982	-0.4019	0.24239	0.14114	-0.8622
ANGLE/R, rad/in	0.01235	0.02072	0.01895	0.02377	0.02888	0.01159
PITCH/FLAP, rd/in	0.01021	0.02034	0.02447	0.02533	0.02782	0.01936
MODAL MASS slg/12	1.915	0.5668	0.721	0.3914	0.4115	1.362
MM * FREQ.SQR	30.8877	16.4981	25.3967	21.9876	24.3372	95.0928

TABLE 12. MODE SHAPES AT STARBOARD HUB FOR JOINED WING #467-AL

CASE	467-AL					
MODE No.	7	8	9	10	11	12
FREQUENCY, Hz.	3.61547	4.24154	4.38105	6.81139	6.9706	9.11271
SYM. OR ASYM.	S	A	S	A	S	A
STARBOARD HUB						
X, in	-0.1204	-0.0073	-0.0487	0.02027	-0.0041	0.13955
Y, in	-0.0720	-0.0121	-0.0351	0.01051	-0.0031	0.15552
Z, in	-0.3148	0.48708	0.45797	-0.0275	0.03766	0.06775
R=SR(X^2+Y^2+Z^2)	0.34471	0.48728	0.46189	0.03576	0.03802	0.21966
X/R	-0.3493	-0.0150	-0.1055	0.56683	-0.1097	0.63529
Y/R	-0.2089	-0.0248	-0.0760	0.29400	-0.0828	0.70799
Z/R	-0.9134	0.99957	0.99150	-0.7695	0.99050	0.30845
X ROT., rad	-0.0036	0.00198	0.00170	0.00171	-0.0012	0.00316
Y ROT., rad	-0.0010	0.00706	0.00693	-0.0008	0.00085	0.00082
Z ROT., rad	0.00193	0.00032	0.00085	-0.0003	0.00006	-0.0023
ANGLE = MOD(ROT)	0.00422	0.00734	0.00718	0.00193	0.00151	0.00401
X ROT / ANGLE	-0.8527	0.26976	0.23656	0.88705	-0.8263	0.78712
Y ROT / ANGLE	-0.2489	0.96189	0.96433	-0.4284	0.56135	0.20616
Z ROT / ANGLE	0.45915	0.04449	0.11867	-0.1719	0.04552	-0.5813
ANGLE/R, rad/in	0.01225	0.01508	0.01556	0.05403	0.03985	0.01829
PITCH/FLAP, rd/in	0.00334	0.01451	0.01513	0.03008	0.02258	0.01222
MODAL MASS,Slg/12	1.664	1.244	1.326	0.2996	0.2996	1.106
MM * FREQ.SQR	21.7511	22.3803	25.4507	13.8999	14.5573	91.8438

TABLE 13. MODE SHAPES AT STARBOARD HUB FOR JOINED WING #467-DH

CASE	467-DH					
MODE No.	7	8	9	10	11	12
FREQUENCY, Hz.	2.64647	3.38915	4.563	7.23255	7.28529	8.41654
SYM. OR ASYM.	S	A	S	A	S	A
STARBOARD HUB						
X, in	-0.0281	0.01383	0.1067	-0.0250	0.01475	-0.0993
Y, in	-0.0484	-0.0050	0.14899	-0.0219	0.02048	-0.2026
Z, in	-0.4797	-0.3066	-0.1470	0.04177	-0.0357	-0.0287
R=SR(X^2+Y^2+Z^2)	0.48296	0.30700	0.23494	0.05343	0.04378	0.22750
X/R	-0.0582	0.04504	0.45415	-0.4686	0.33691	-0.4367
Y/R	-0.1003	-0.0165	0.63415	-0.4111	0.46790	-0.8906
Z/R	-0.9932	-0.9988	-0.6257	0.78187	-0.8170	-0.1264
X ROT., rad	-0.0029	-0.0005	0.00108	-0.0018	0.00145	-0.0021
Y ROT., rad	-0.0038	-0.0043	-0.0032	0.00098	-0.0007	-0.0002
Z ROT., rad	0.00061	-0.0002	-0.0017	0.00040	-0.0002	0.00217
ANGLE = MOD(ROT)	0.00488	0.00438	0.00388	0.00212	0.00166	0.00304
X ROT / ANGLE	-0.6057	-0.1144	0.28020	-0.8639	0.87440	-0.6952
Y ROT / ANGLE	-0.7854	-0.9922	-0.8416	0.46590	-0.4633	-0.0768
Z ROT / ANGLE	0.12662	-0.0490	-0.4616	0.19127	-0.1439	0.71465
ANGLE/R, rad/in	0.01010	0.01427	0.01654	0.03971	0.03797	0.01340
PITCH/FLAP, rd/in	0.00799	0.01417	0.02225	0.02366	0.02153	0.00814
MODAL MASS,Slg/12	2.015	0.7433	0.8786	0.2996	0.2814	1.021
MM * FREQ.SQR	14.1126	8.53779	18.2933	15.6720	14.9354	72.3257

TABLE 14. MODE SHAPES AT STARBOARD HUB FOR JOINED WING #468-AL

CASE	468-AL					
MODE No.	7	8	9	10	11	12
FREQUENCY, Hz.	3.19094	4.26368	4.3788	7.07945	7.31556	9.26524
SYM. OR ASYM.	S	A	S	A	S	A
STARBOARD HUB						
X, in	0.1133	0.01267	0.02825	-0.0237	-0.0035	-0.1186
Y, in	0.04092	0.01632	0.01838	-0.0137	-0.0024	-0.1254
Z, in	0.24089	-0.4852	-0.4863	0.01529	0.03231	-0.0809
R=SR(X^2+Y^2+Z^2)	0.26933	0.48565	0.48754	0.03141	0.03259	0.19070
X/R	0.42067	0.02608	0.05795	-0.7550	-0.1074	-0.6220
Y/R	0.15193	0.03362	0.03771	-0.4392	-0.0750	-0.6579
Z/R	0.89440	-0.9990	-0.9976	0.48674	0.99137	-0.4245
X ROT., rad	0.00328	-0.0021	-0.0024	-0.0019	-0.0013	-0.0030
Y ROT., rad	-0.0002	-0.0071	-0.0069	0.00063	0.00075	-0.0010
Z ROT., rad	-0.0018	-0.0004	-0.0005	0.00039	0.00006	0.00205
ANGLE = MOD(ROT)	0.00375	0.00742	0.00733	0.00209	0.00156	0.00380
X ROT / ANGLE	0.87415	-0.2868	-0.3314	-0.9342	-0.8747	-0.7936
Y ROT / ANGLE	-0.0558	-0.9562	-0.9407	0.30170	0.48294	-0.2812
Z ROT / ANGLE	-0.4824	-0.0576	-0.0721	0.19010	0.03972	0.53945
ANGLE/R, rad/in	0.01394	0.01529	0.01505	0.06675	0.04800	0.01996
PITCH/FLAP, rd/in	-0.0008	0.01463	0.01419	0.04137	0.02338	0.01322
MODAL MASS,Slg/12	1.699	1.251	1.277	0.2818	0.267	0.9144
MM * FREQ.SQR	17.2993	22.7418	24.4850	14.1234	14.2891	78.4963

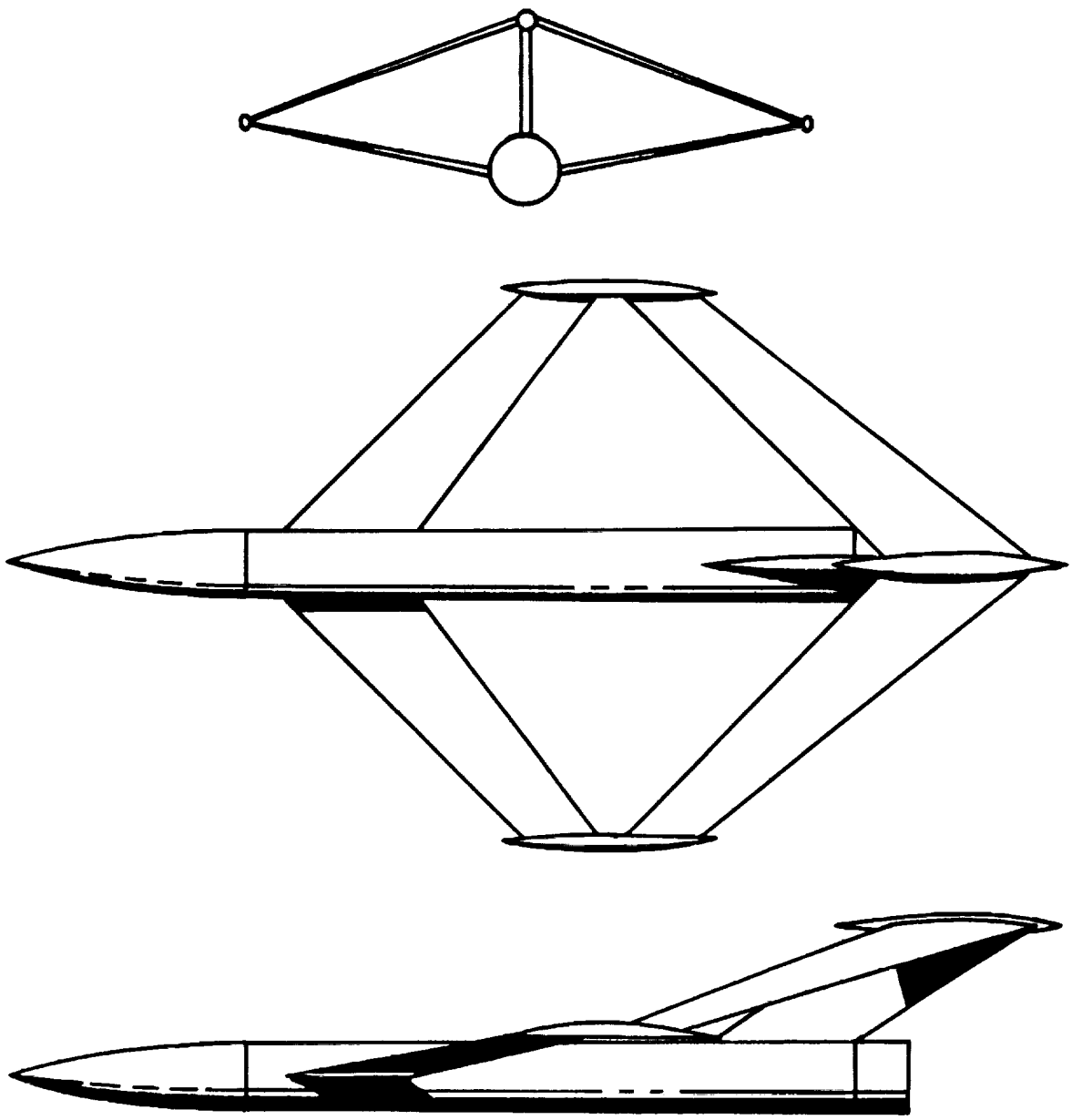

Fig. 1. Joined Wing Configuration with Tip Joint

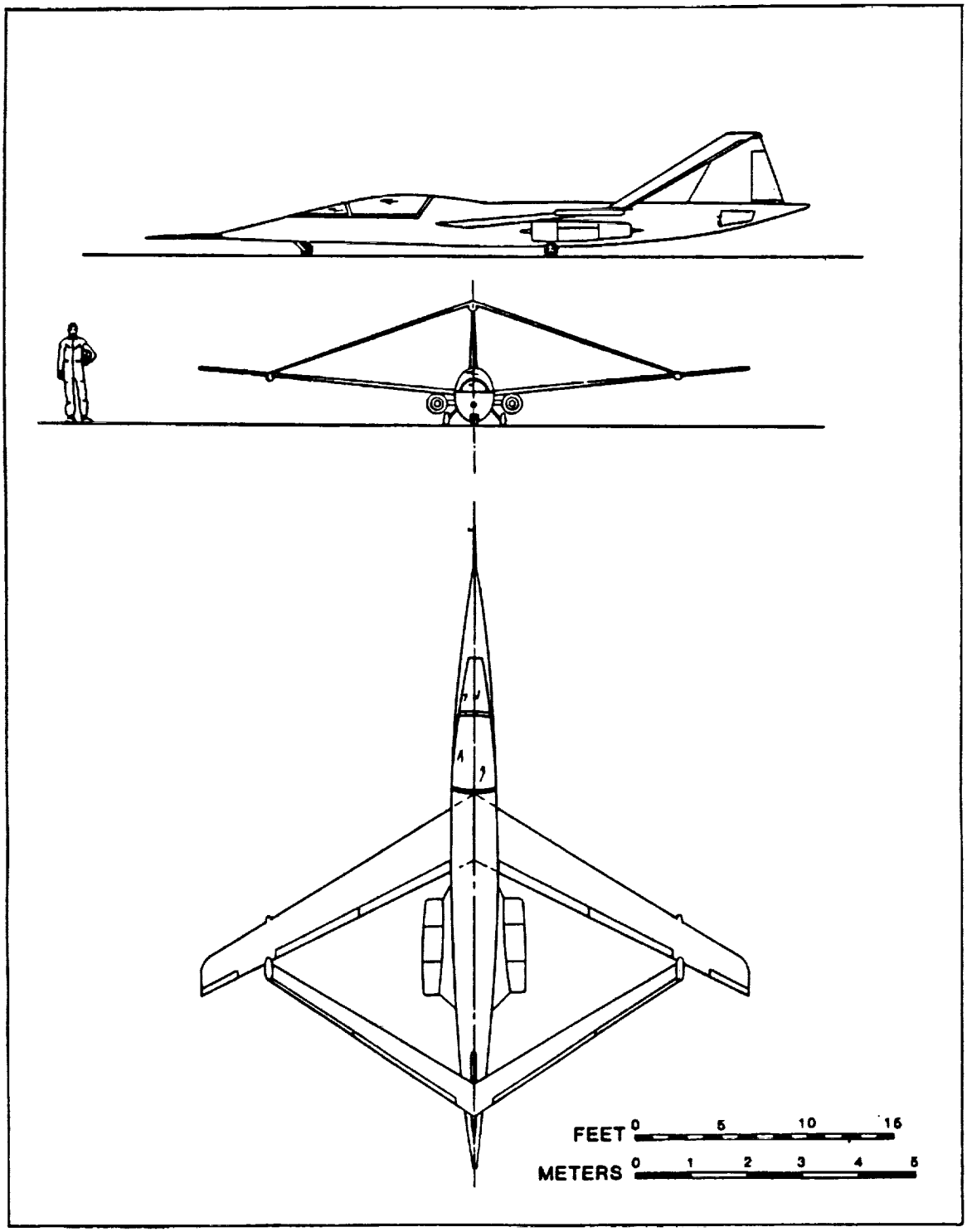

JOINED WING RESEARCH AIRPLANE
WITH JOINT AT 80 PERCENT OF SPAN

Fig. 2. Joined Wing Configuration with Inboard Joint

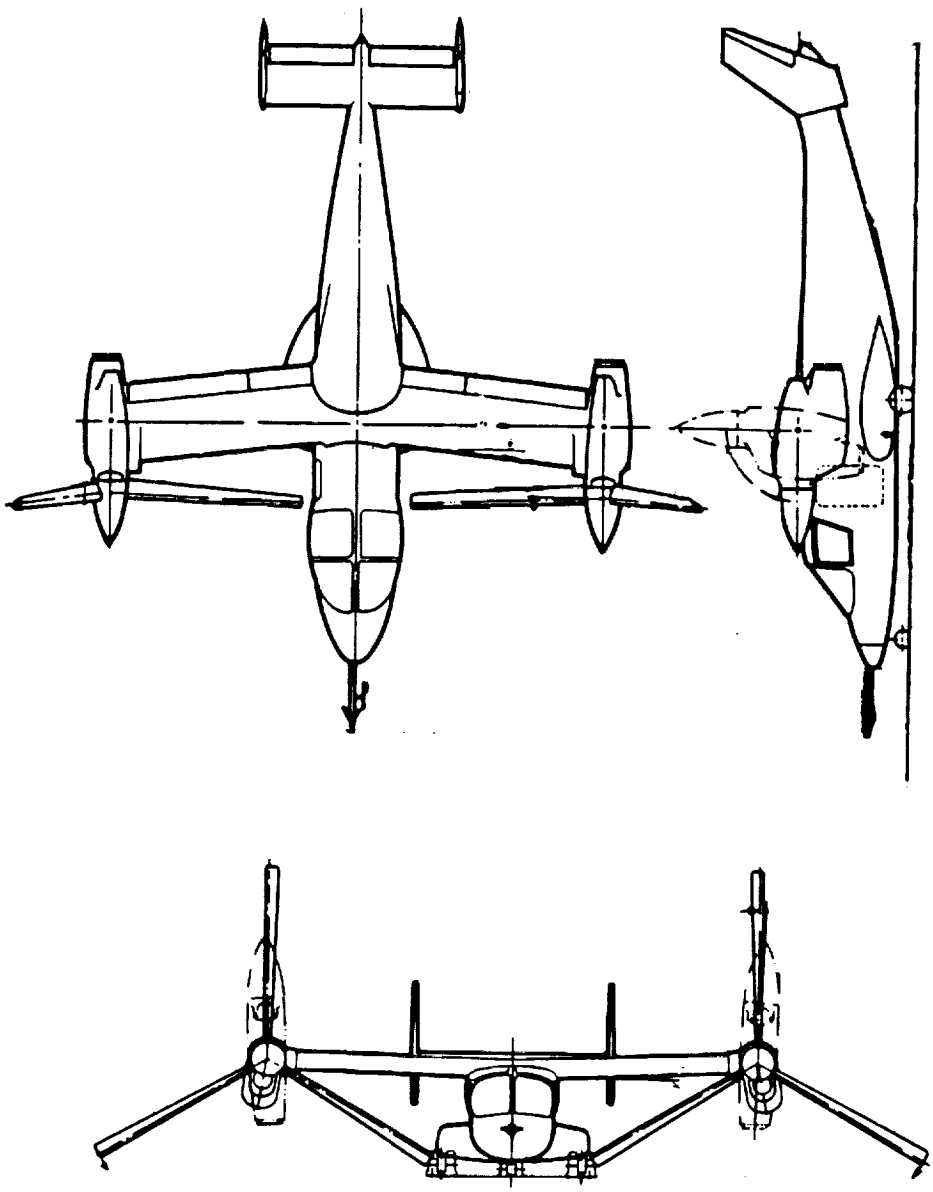

Fig. 3. XV-15 Tiltrotor Aircraft General Arrangement

ORIGINAL PAGE
BLACK AND WHITE PHOTOGRAPH

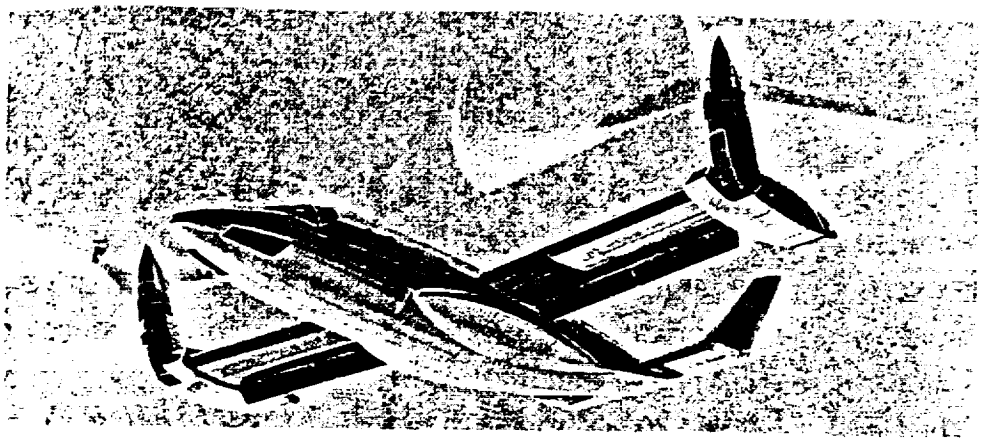

Fig. 4. Tiltrotor with Fixed Nacelles and Tilting Shafts

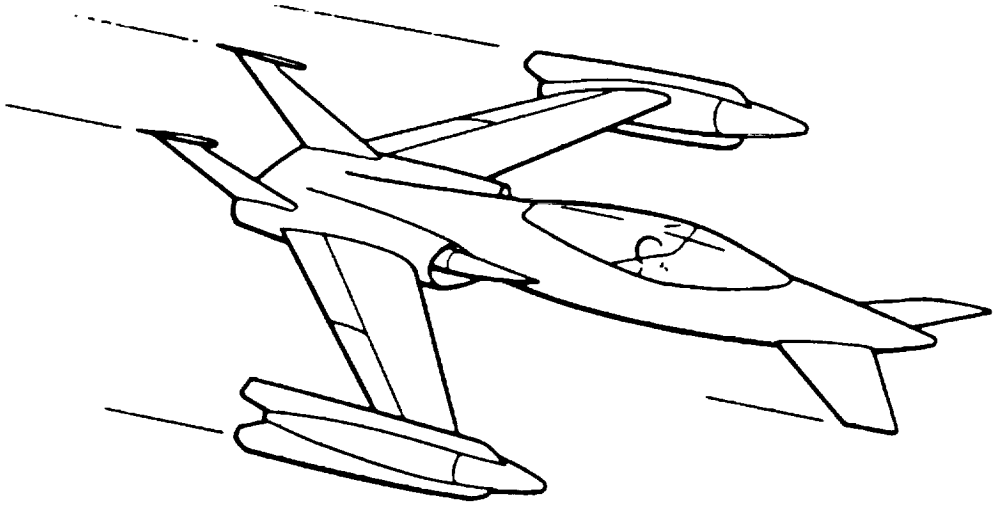

Fig. 5. Folding Tiltrotor Configuration

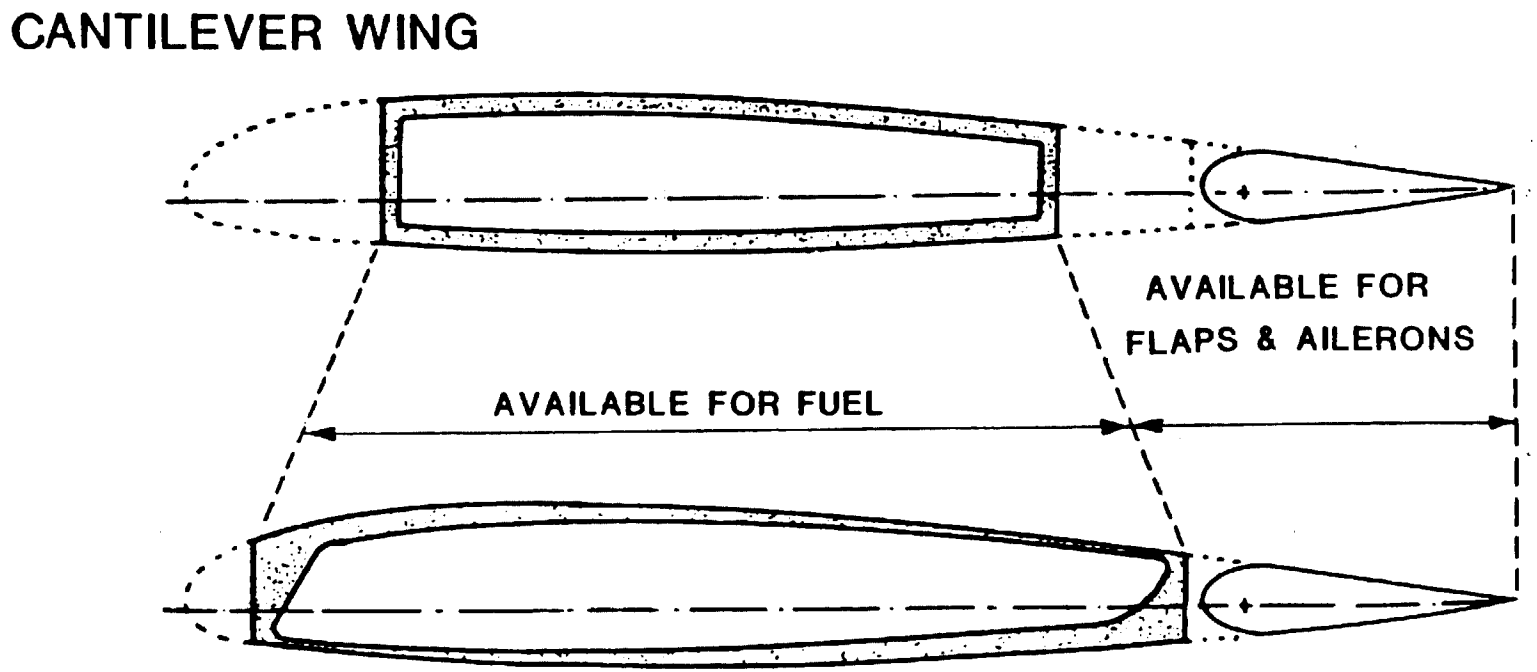

Fig. 6. Comparison of Optimum Structural Material Distributions for Cantilever and Joined Wings

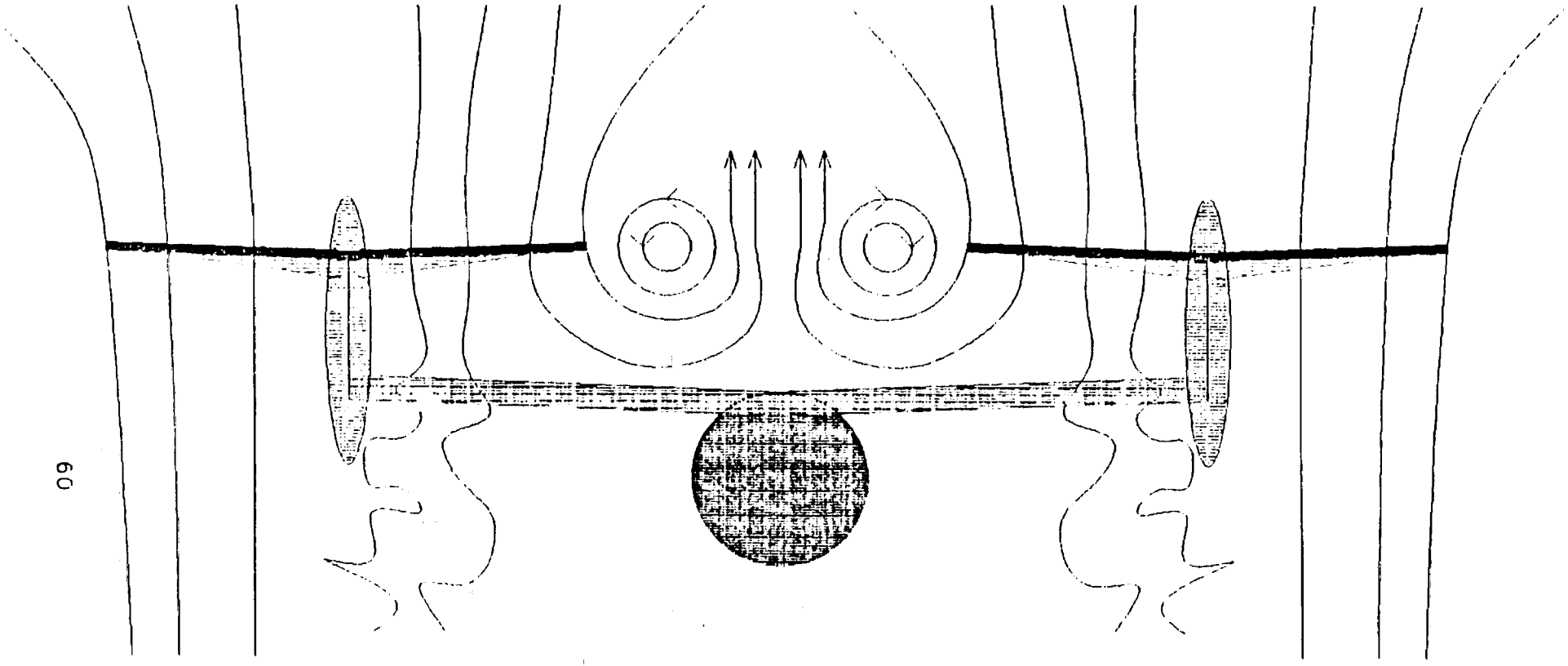

Fig. 7. Downwash Recirculation in Hover

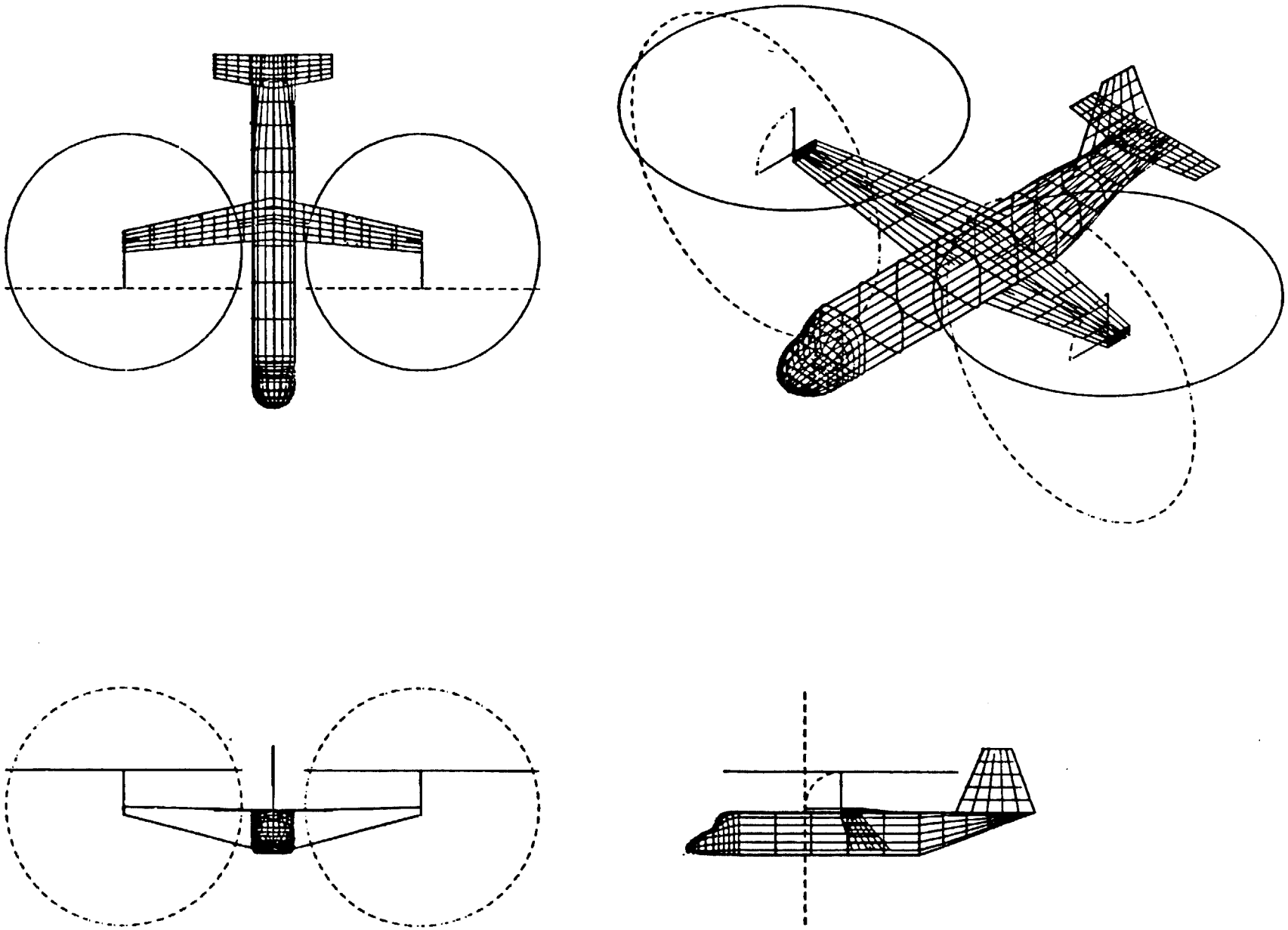

Fig. 8. Joined Wing Configuration with Unstaggered Wings

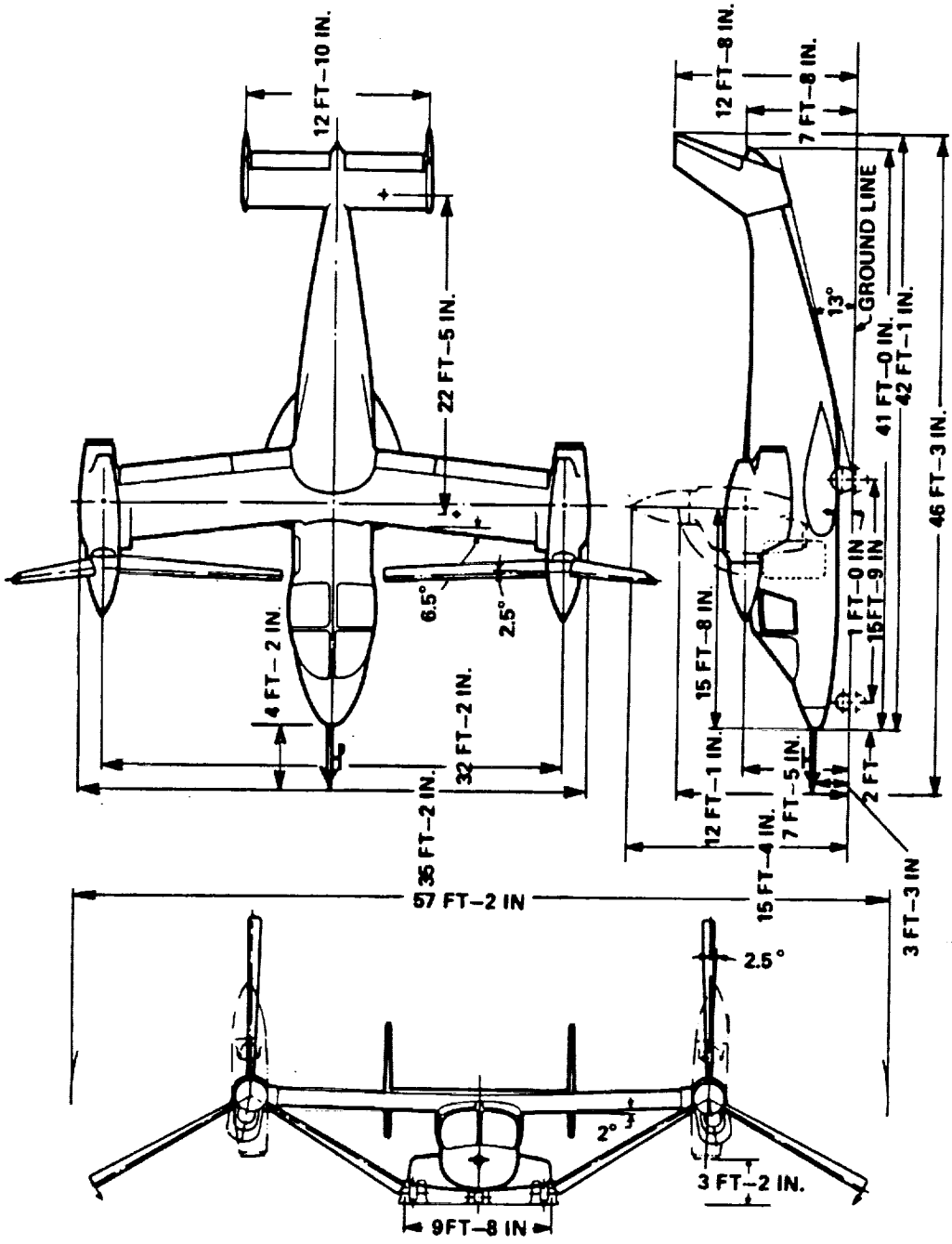

Fig. 9. XV-15 Dimensions and Detailed Geometry

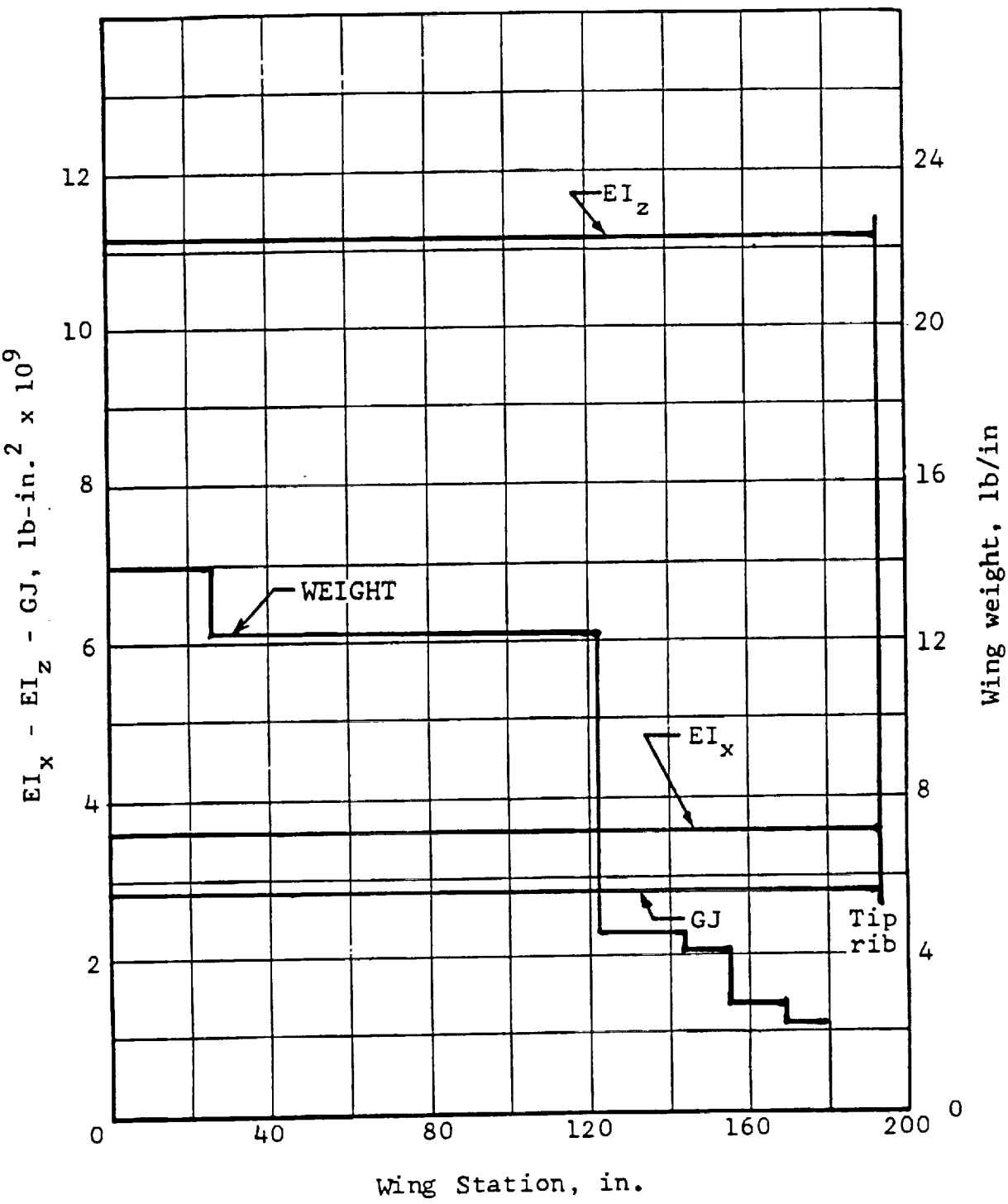

Fig. 10. XV-15 Wing Structural and Mass Characteristics

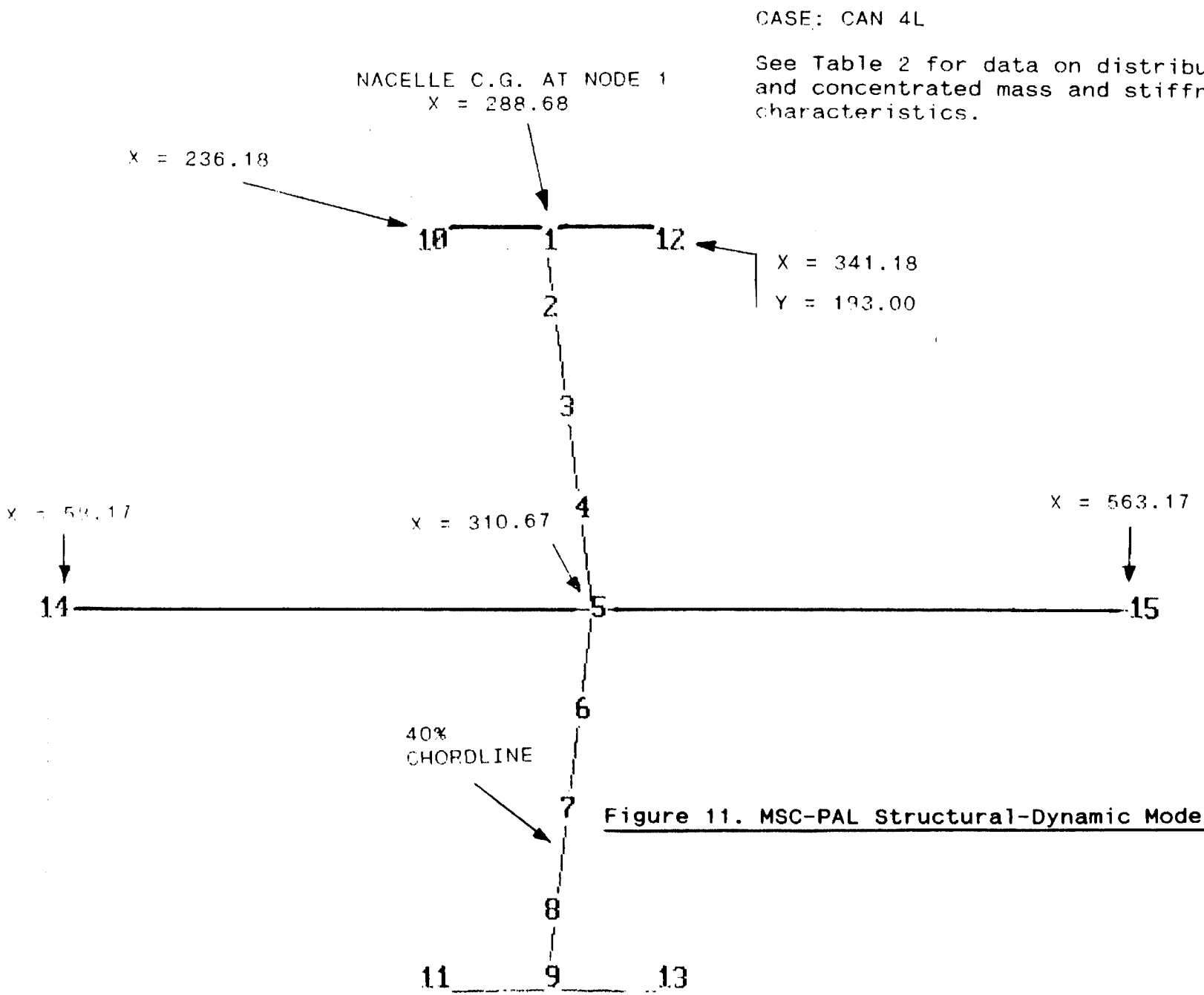

Figure 11. MSC-PAL Structural-Dynamic Model of XV-15.

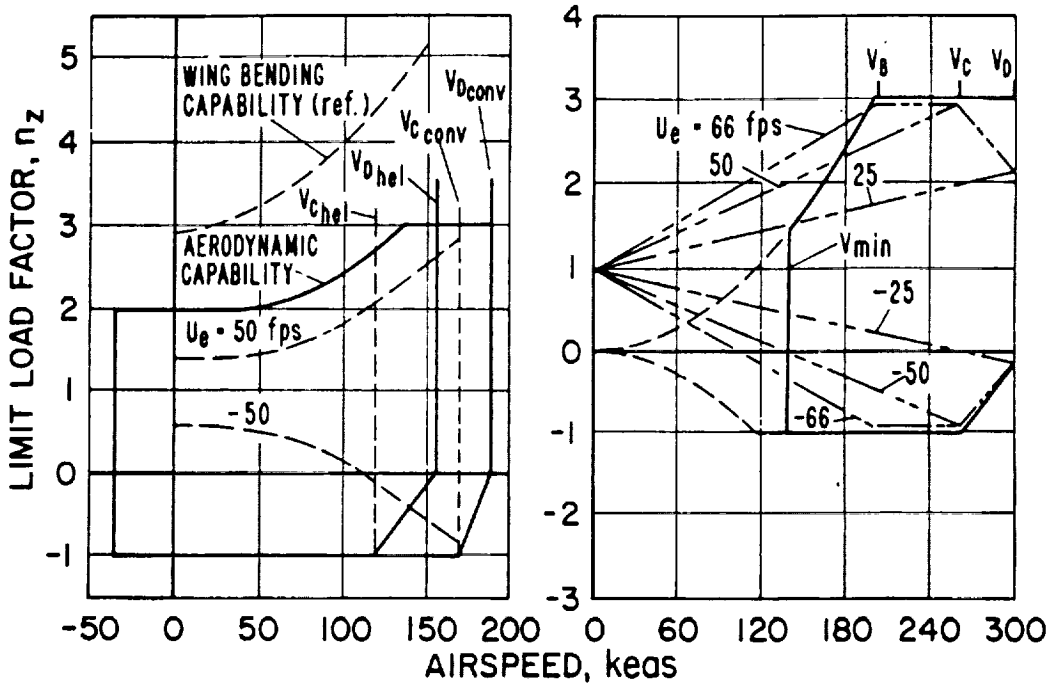

V-n diagram, design gross weight, 13,000 pounds.

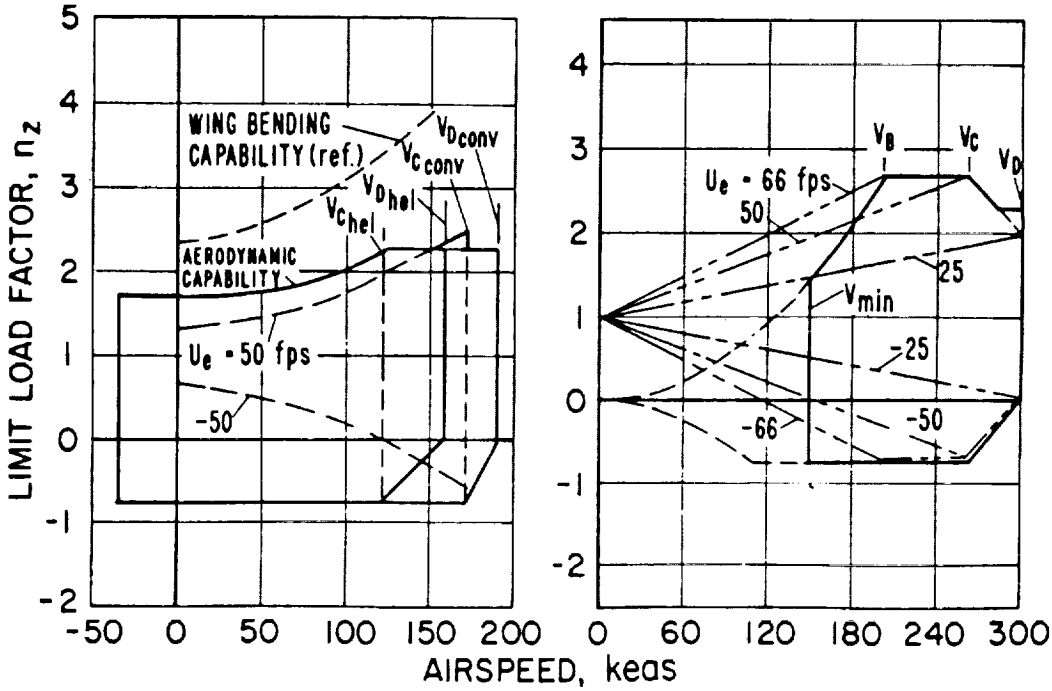

V-n diagram, maximum gross weight, 15,000 pounds

Fig. 12. XV-15 Flight Envelope

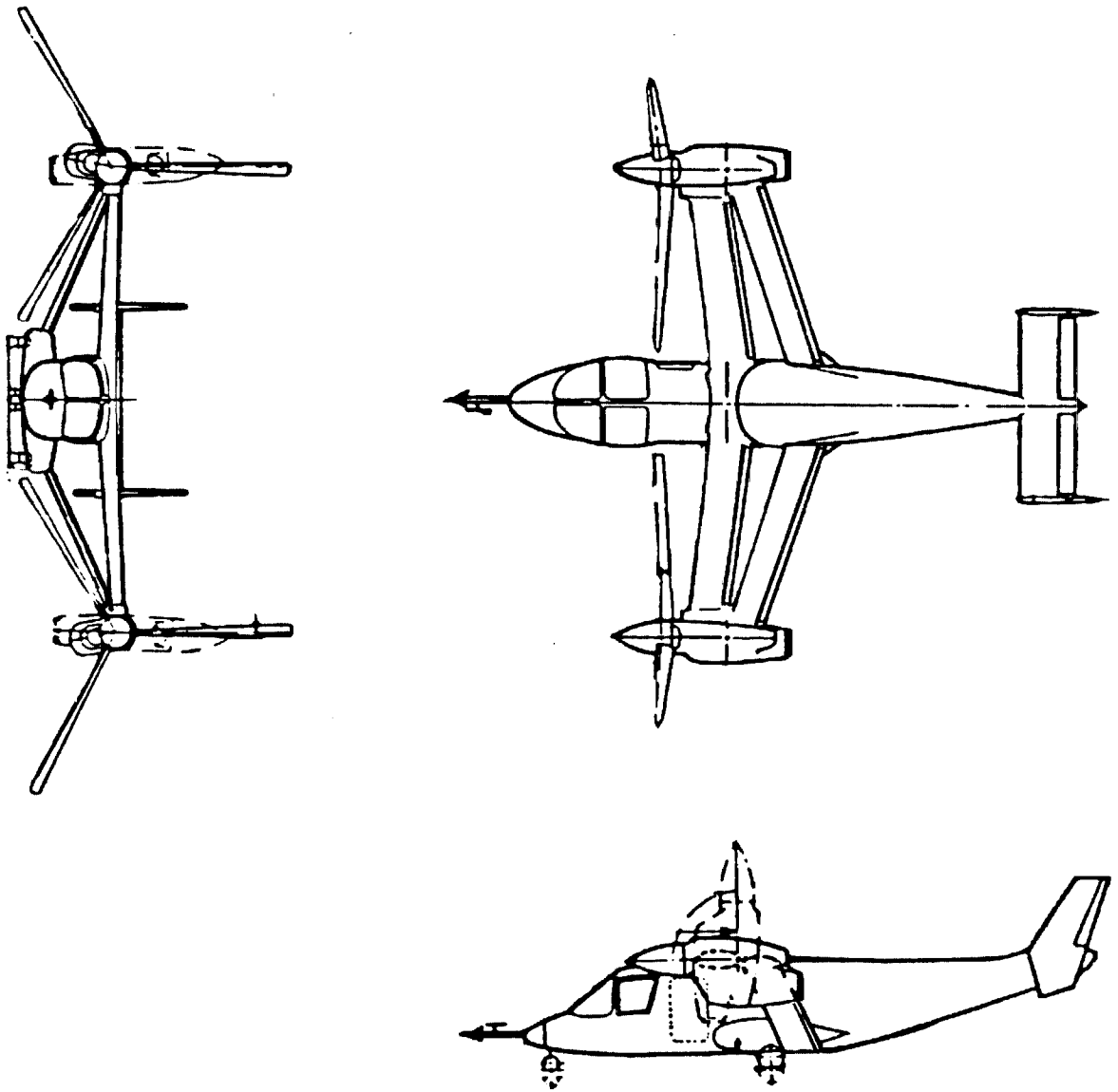

Fig. 13. Joined-Wing Tiltrotor Configuration 166AL

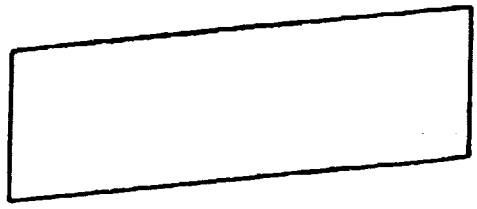

XV-15

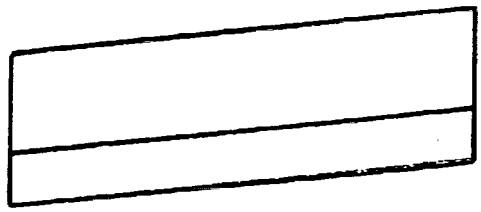

REAR WING SWEEP: -6.5 DEG

REAR WING SWEEP: -15 DEG

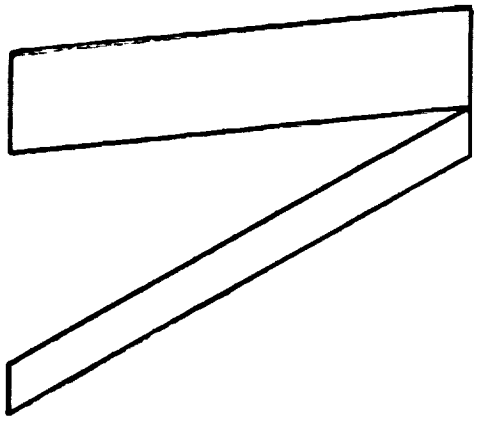

REAR WING SWEEP: -30 DEG

Fig. 14. Plan Views of Configurations Studied With Front Wing Sweep = -6.5 Degrees

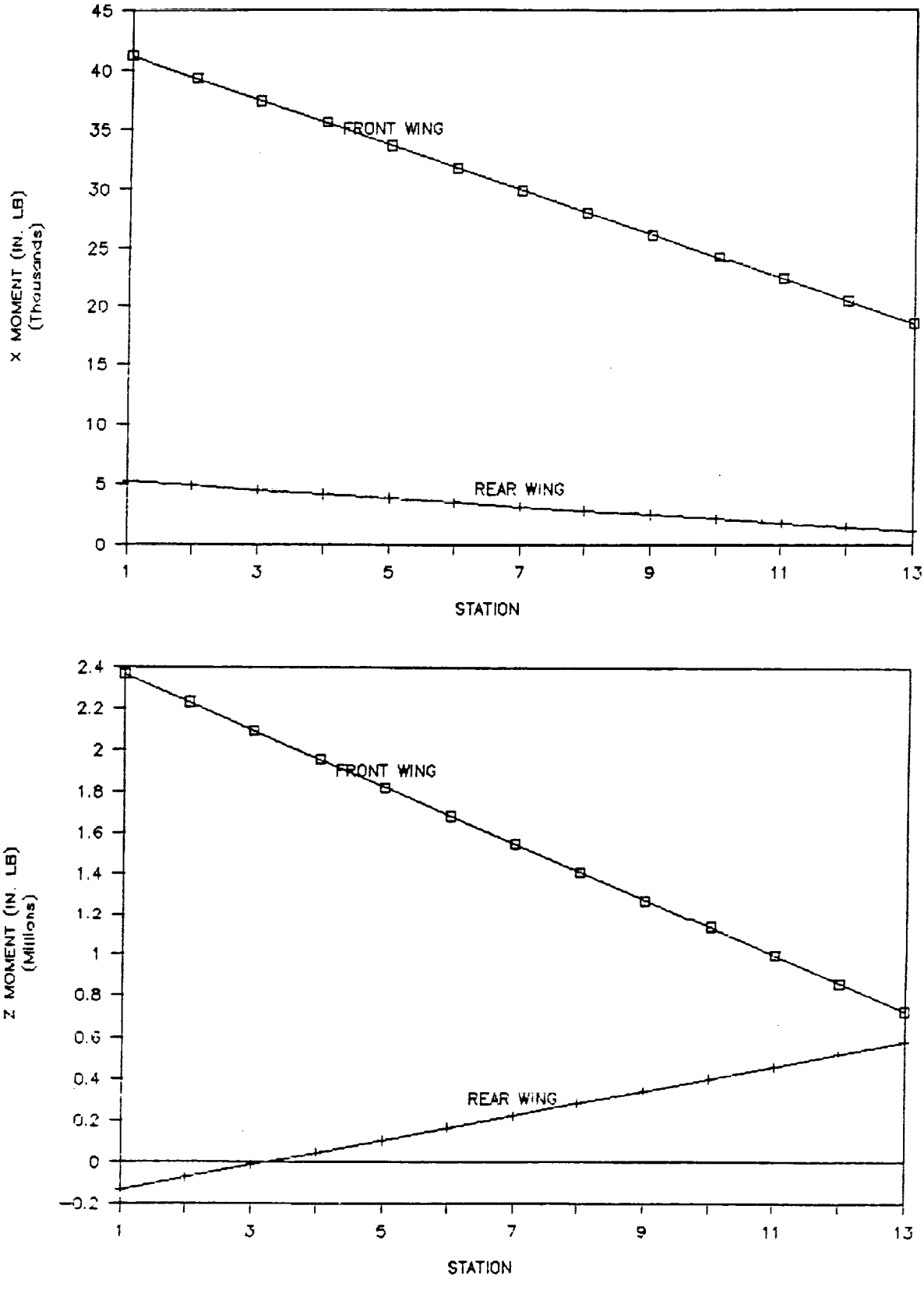

Fig. 15. Beam and Chordwise Design Bending Moments for Joined-Wing Tiltrotor Configuration 166AL

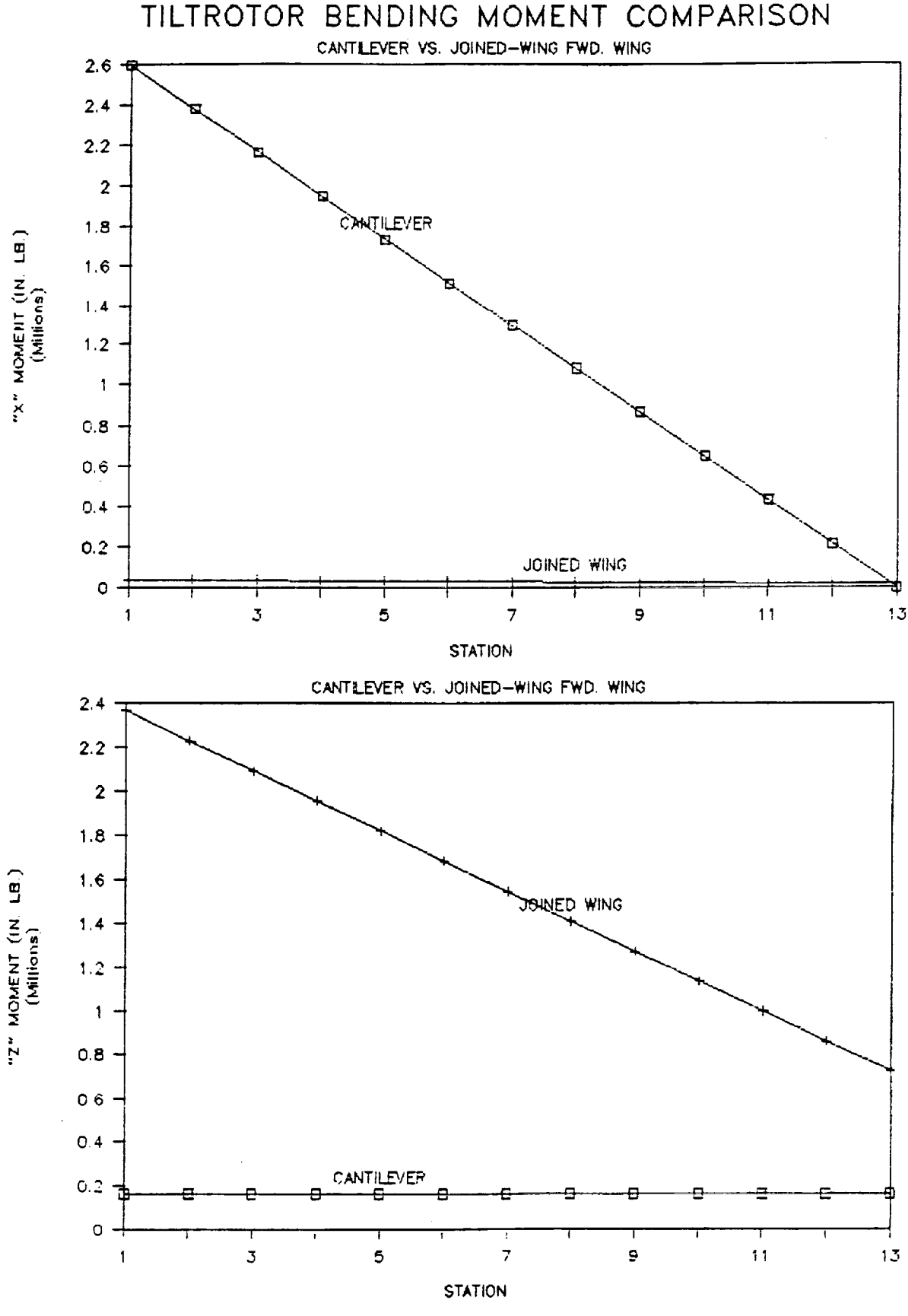

Fig. 16. Comparison of Bending Moments for Joined and Cantilever Wings

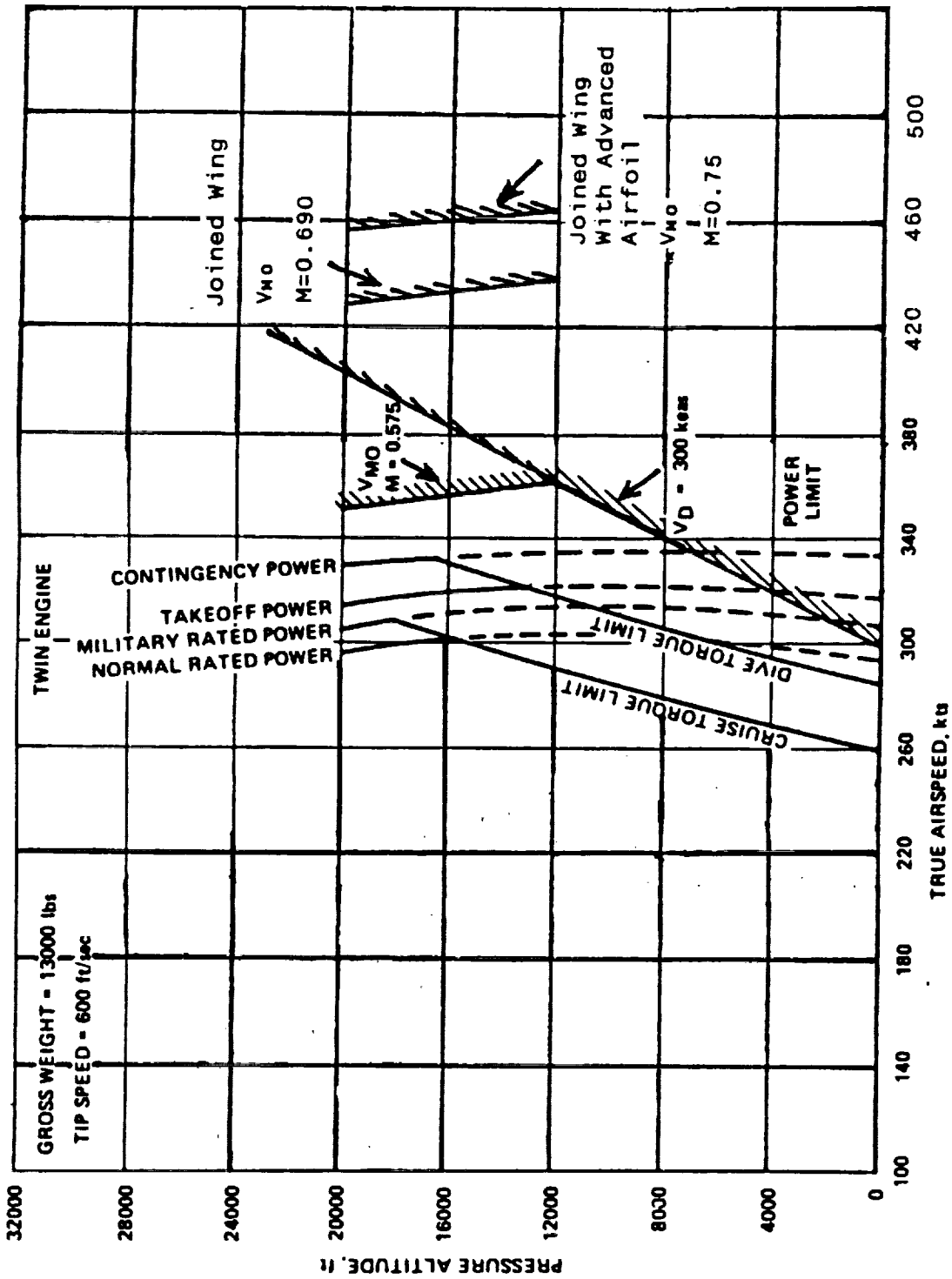

Fig. 17. Effect of Joined Wing on Speed Capability

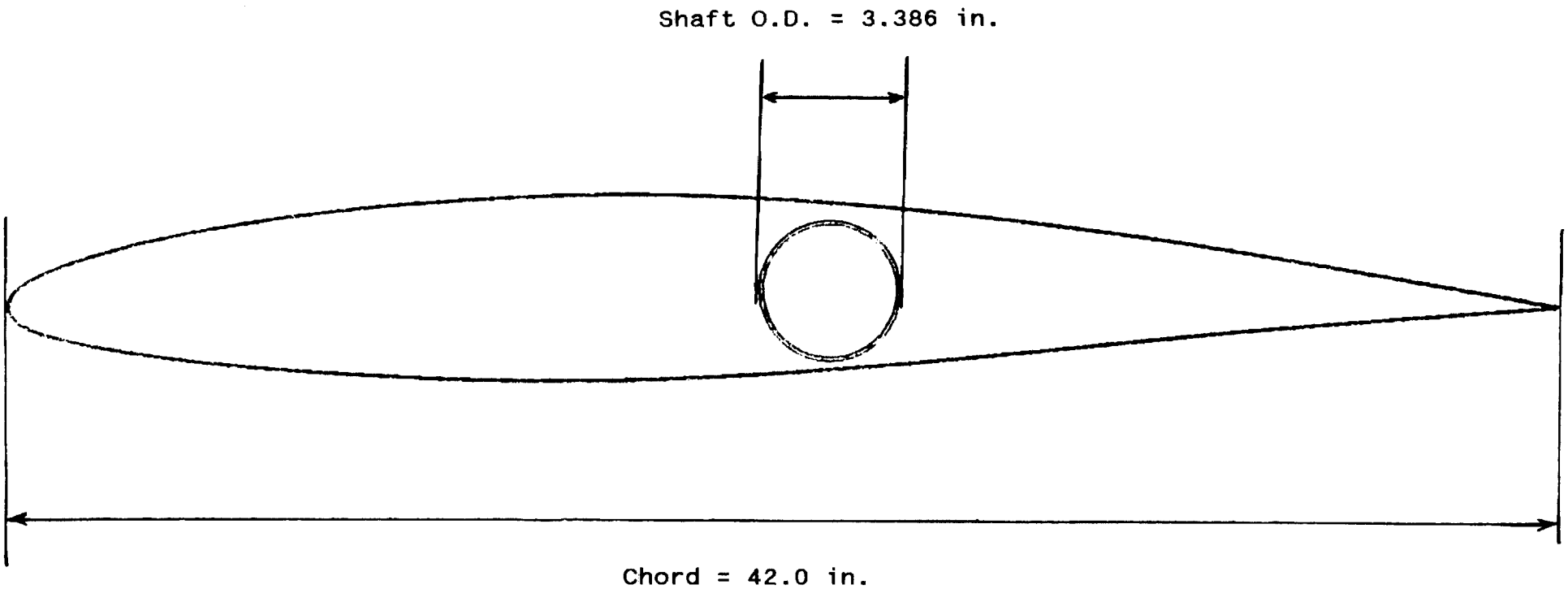

Fig. 18. Accommodation of Cross-Shaft Within Front Wing

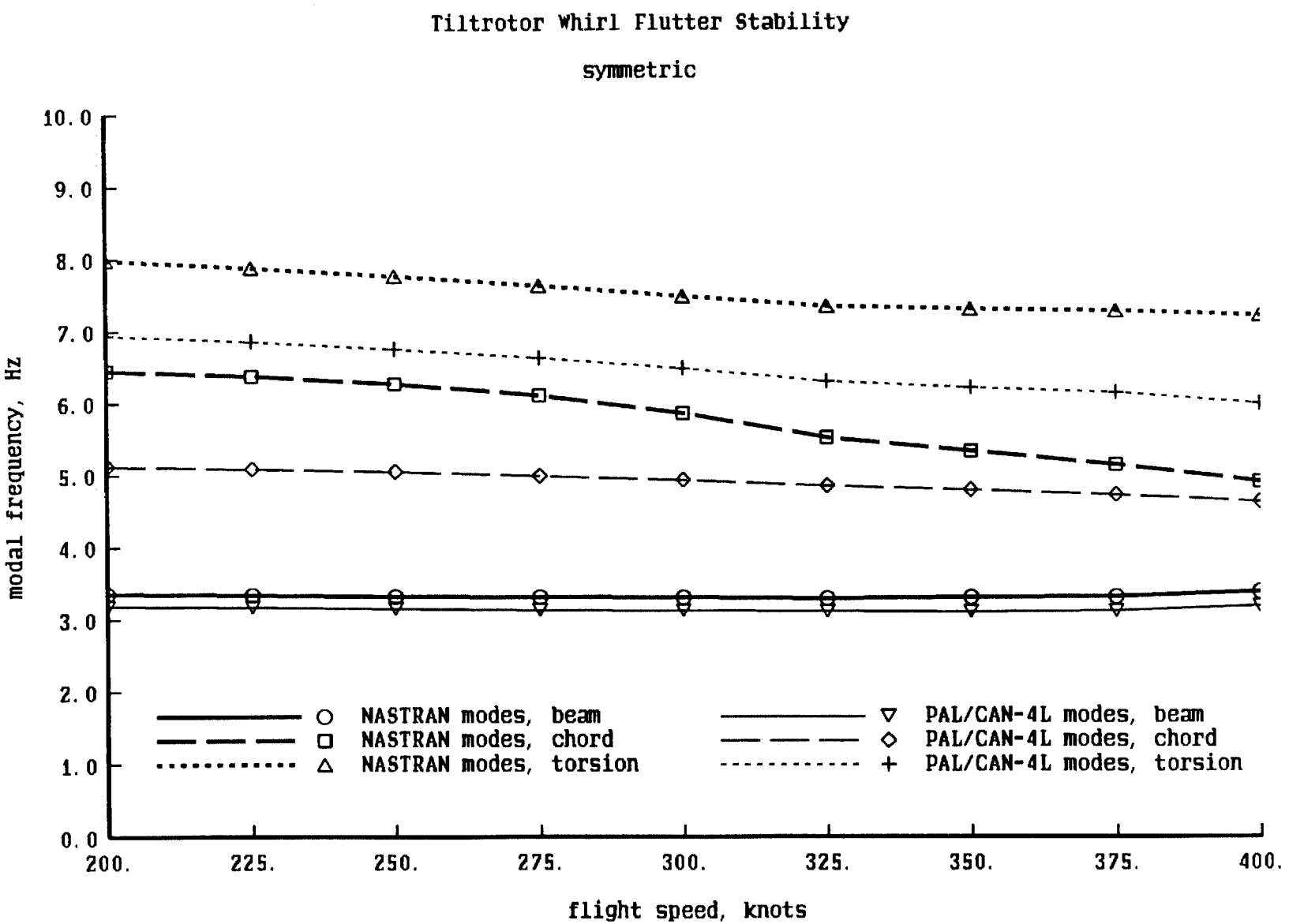

Fig. 19. Frequencies of XV-15 Symmetric Modes versus EAS

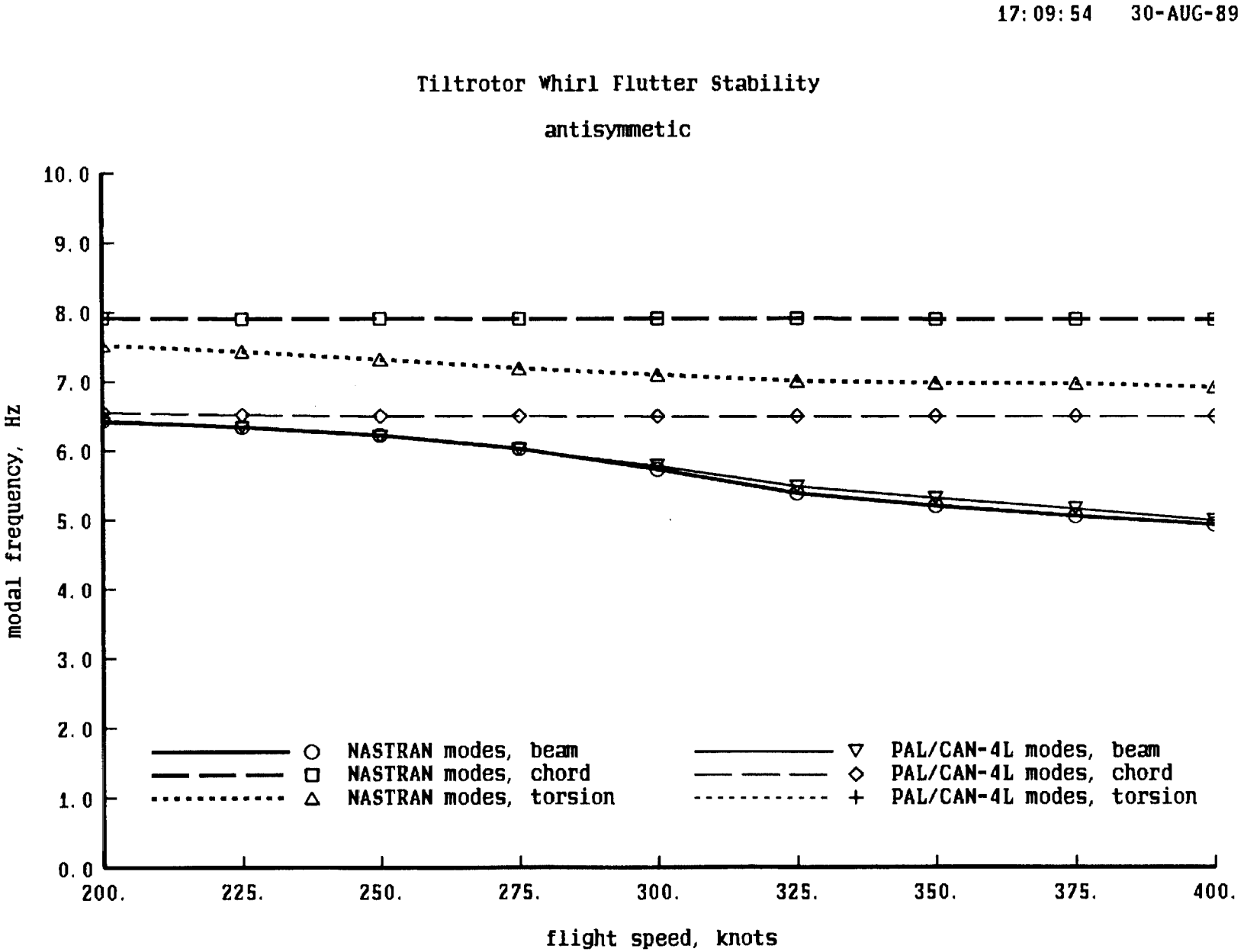

Fig. 20. Frequencies of XV-15 Antisymmetric Modes versus EAS

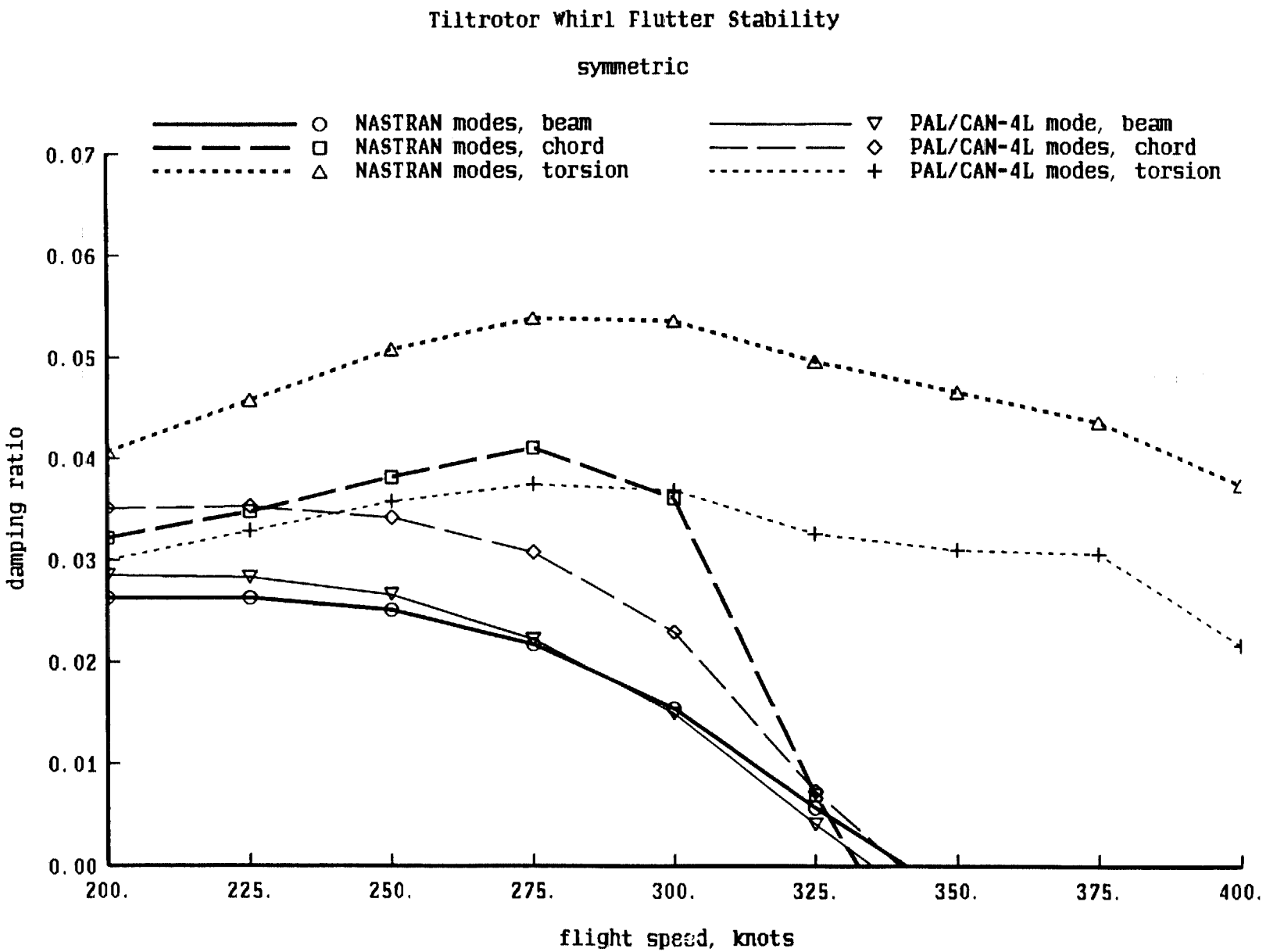

Fig. 21. Damping of XV-15 Symmetric Modes versus EAS

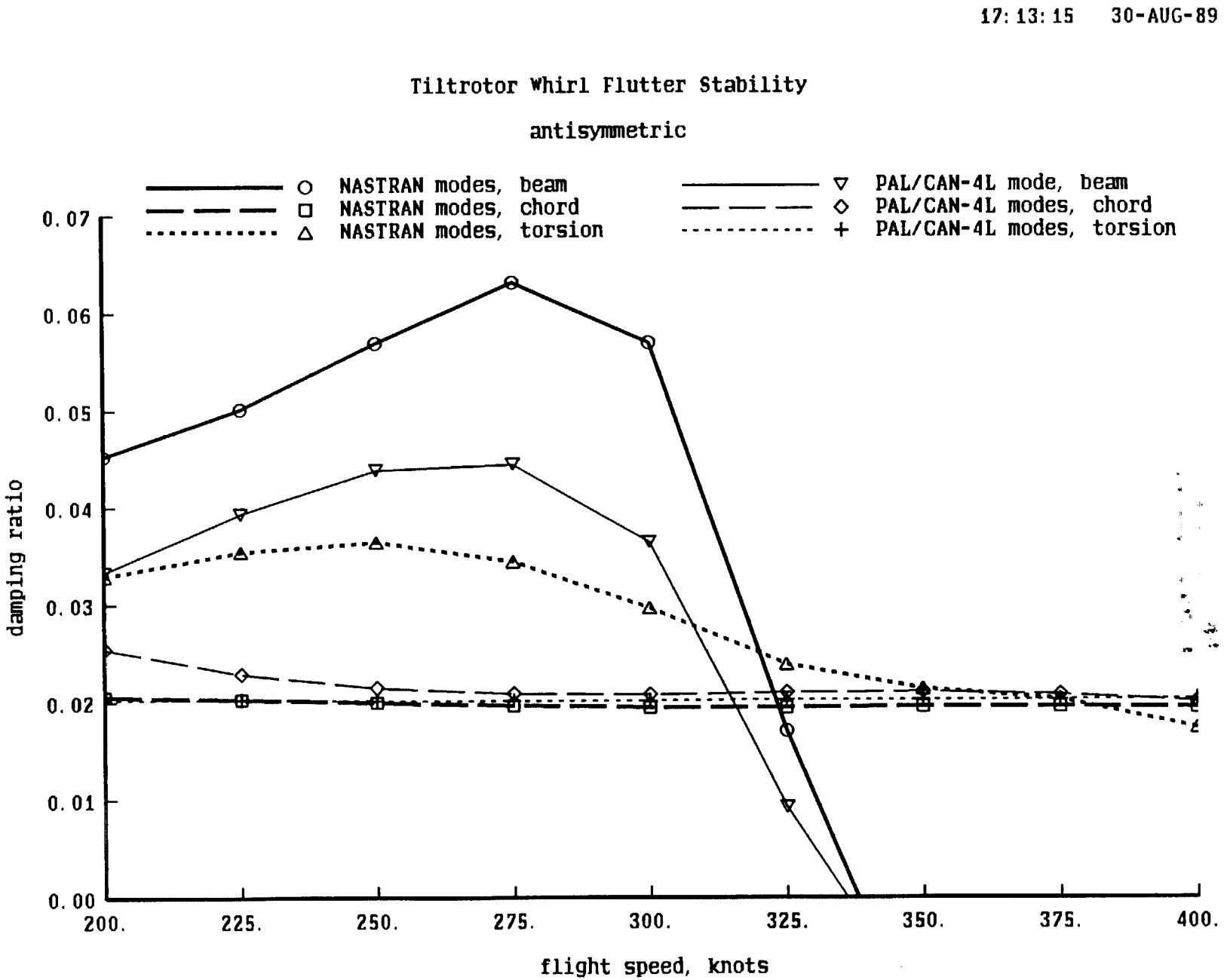

Fig. 22. Damping of XV-15 Antisymmetric Modes versus EAS

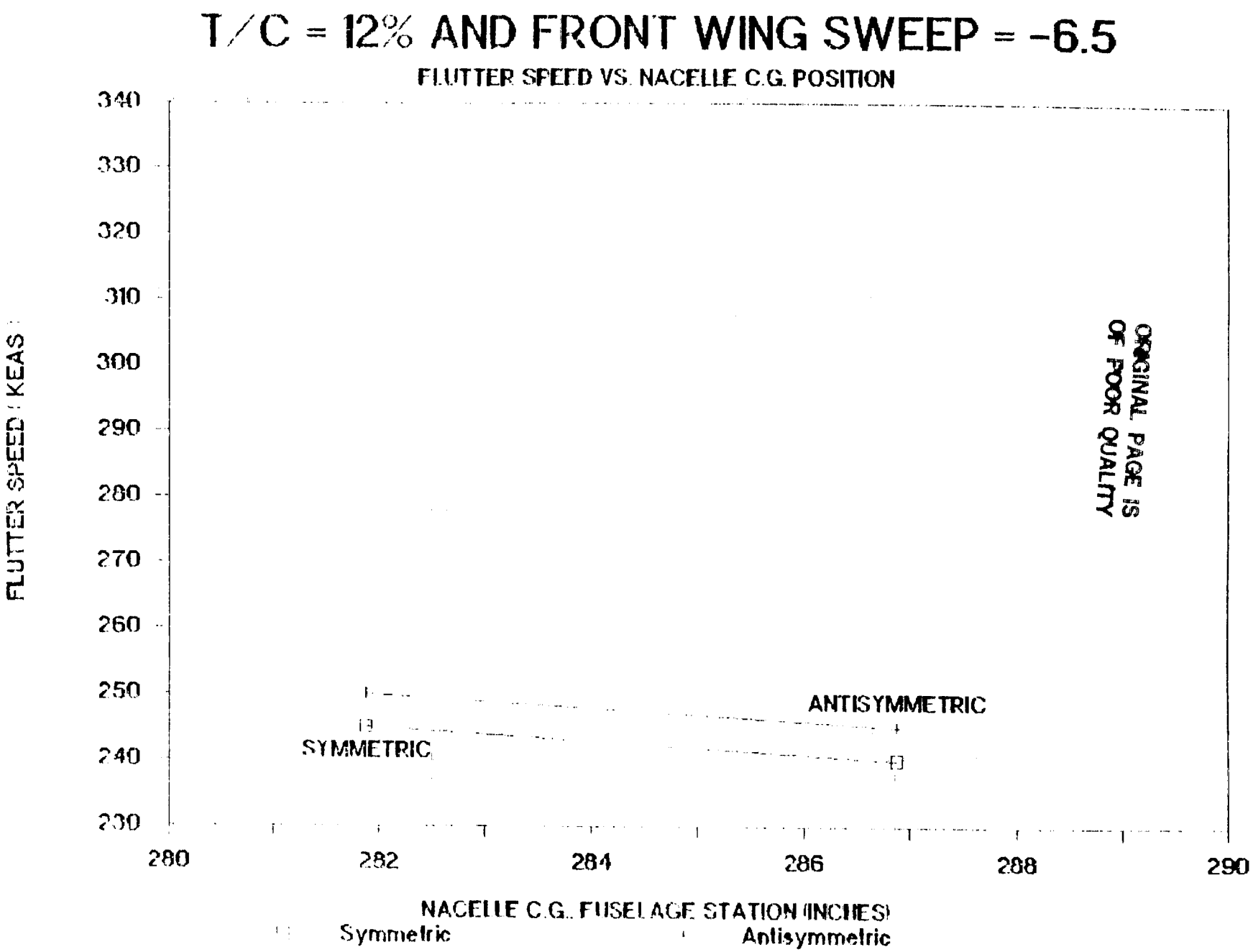

Fig. 23. Flutter Speed vs. Nacelle C.G. Position

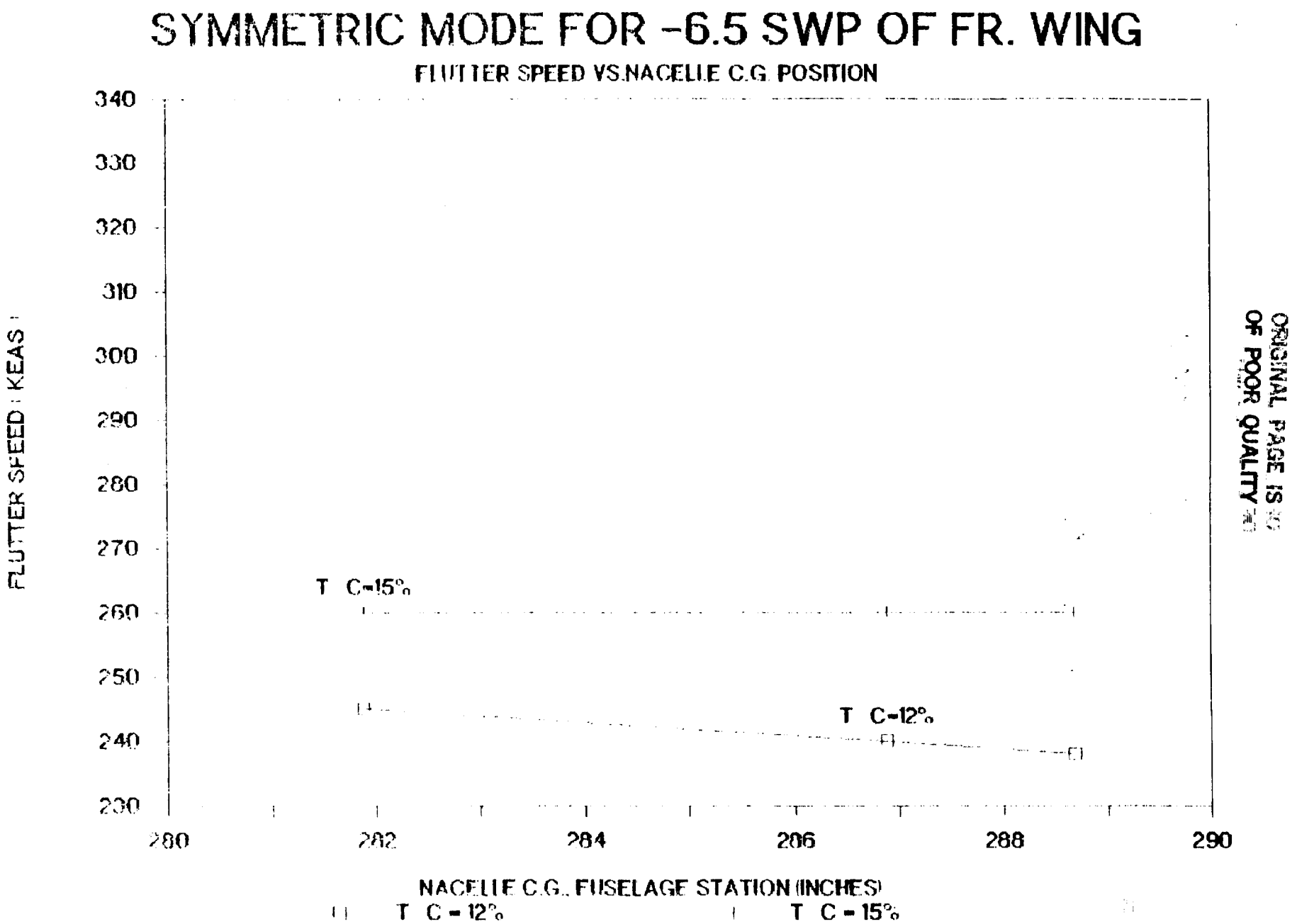

Fig. 24. Effect of a 3% Increase in the Thickness of the Front Wing on Flutter Speed of the First Symmetric Mode

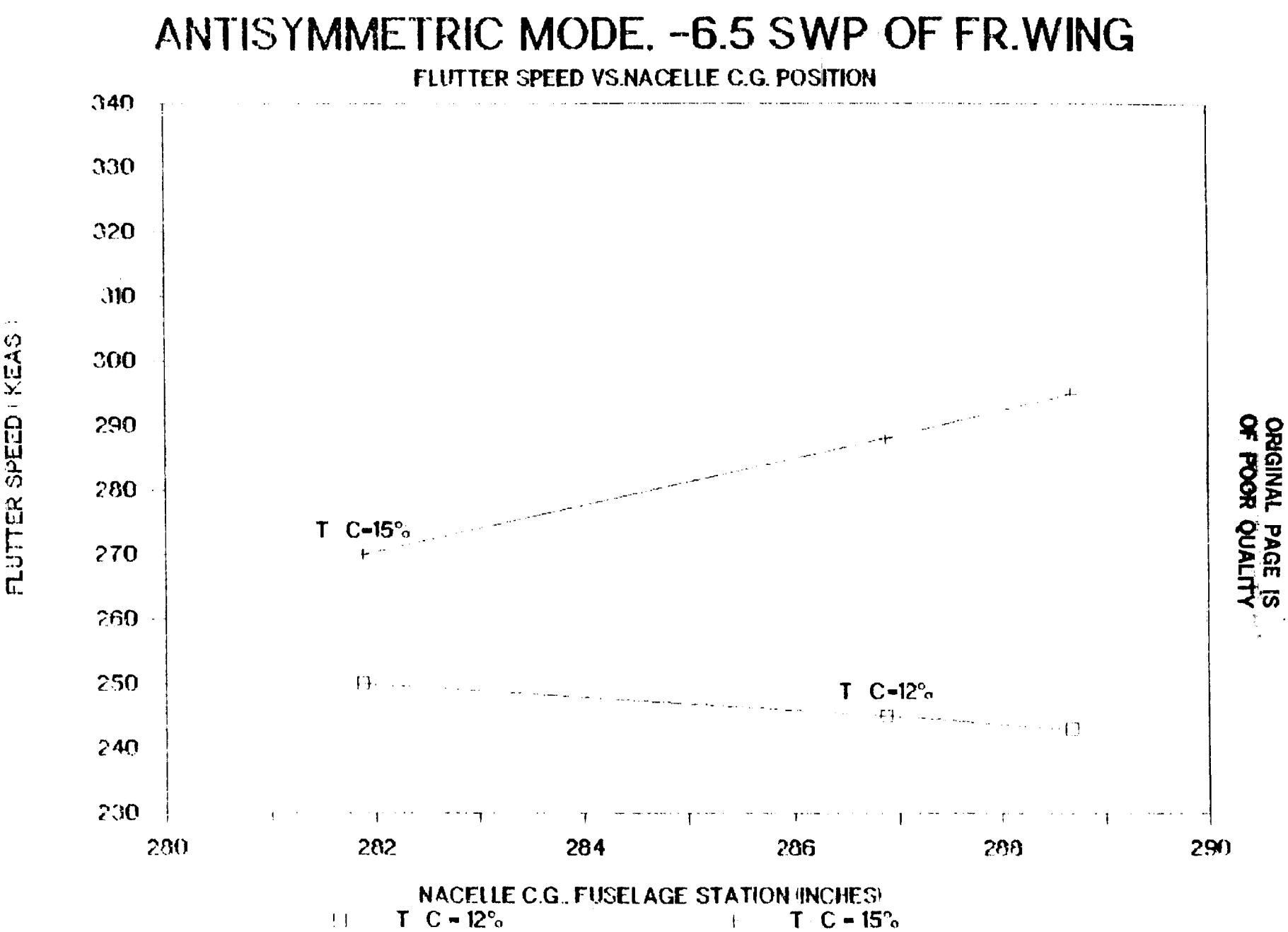

Fig. 25. Effect of a 3% Increase in the Thickness of the Front Wing on Flutter Speed of the First Antisymmetric Mode

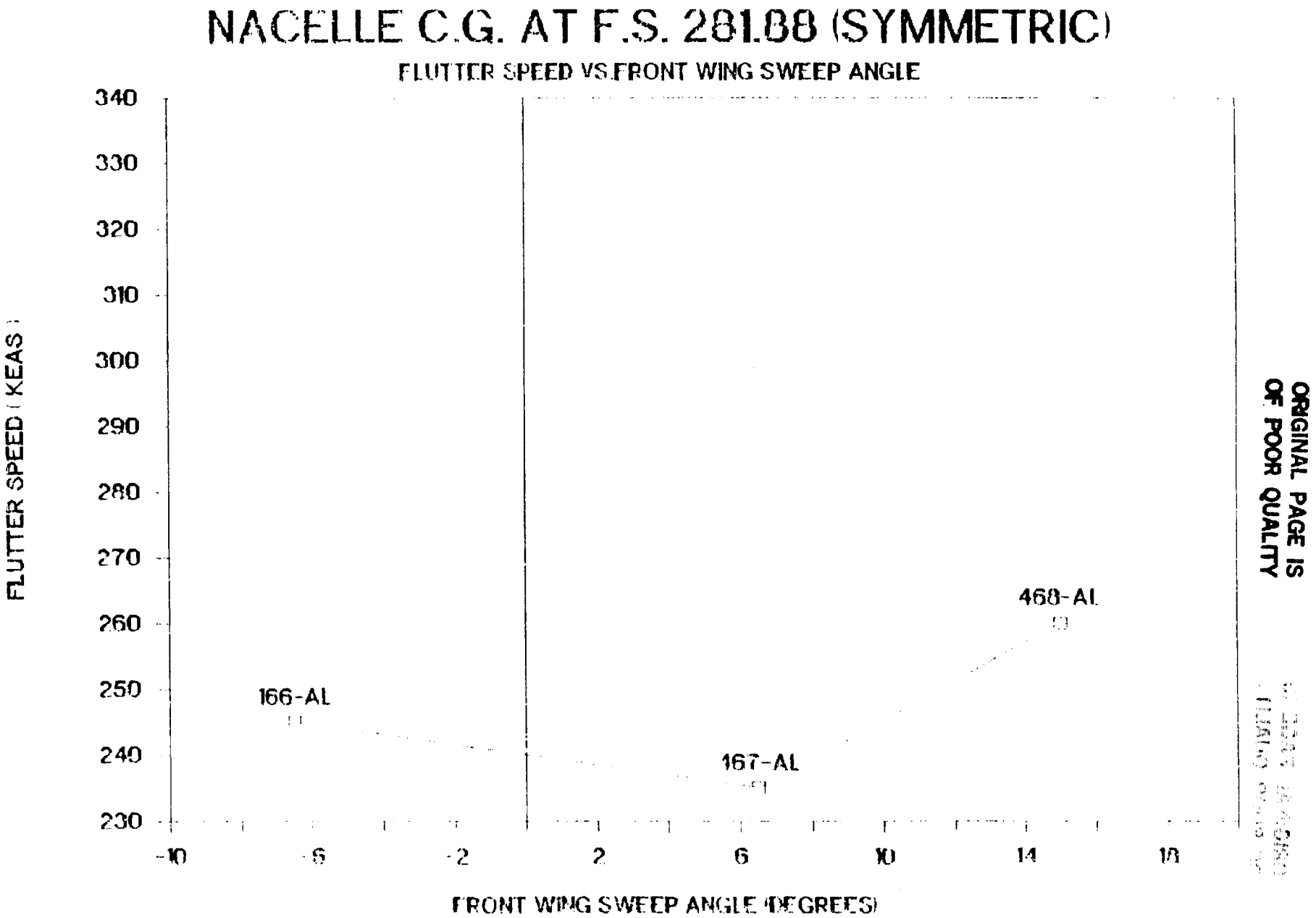

Fig. 26. Effect of Sweep on Flutter Speed of First Symmetric Mode

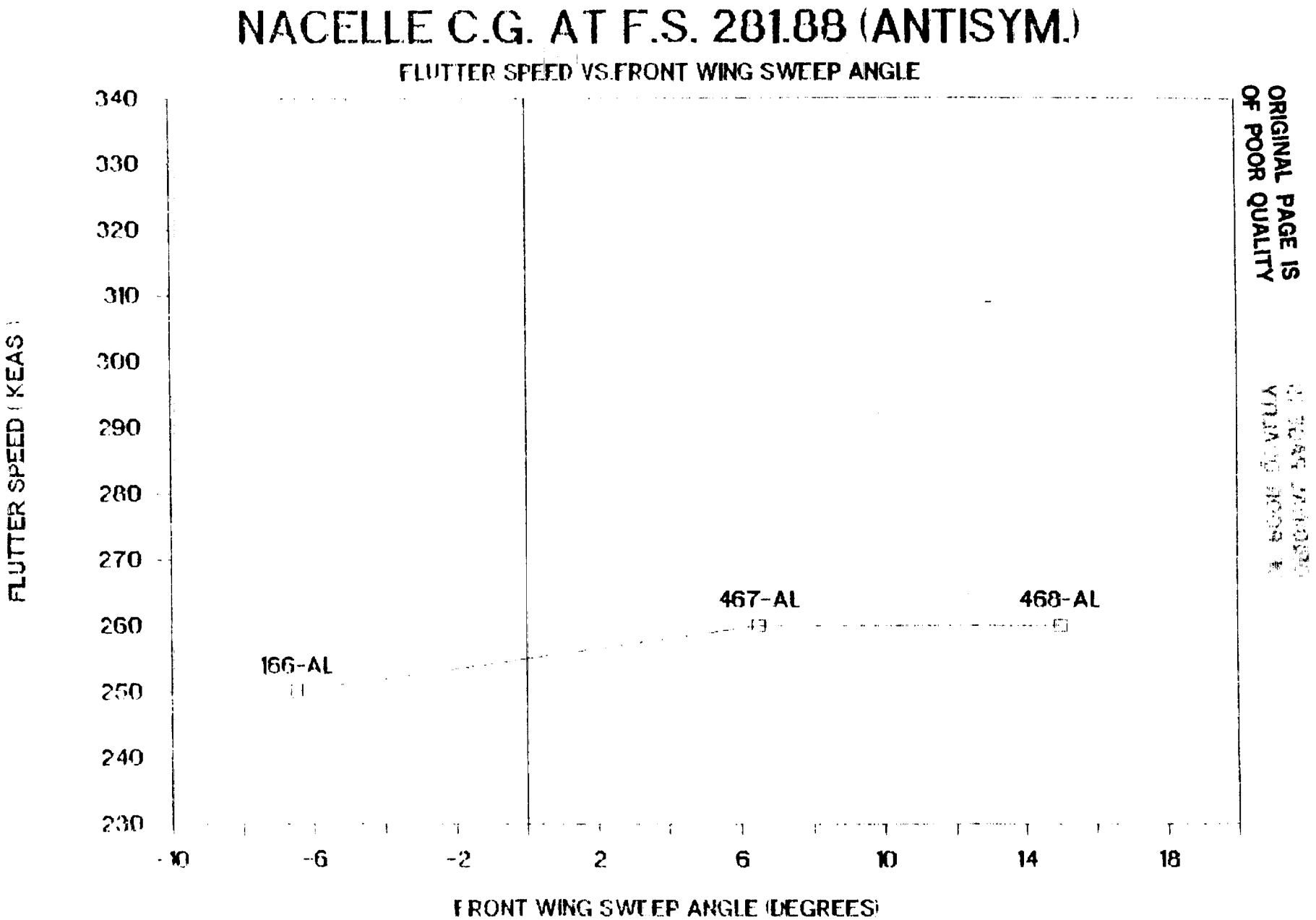

Fig. 27. Effect of Sweep on Flutter Speed of First Antisymmetric Mode

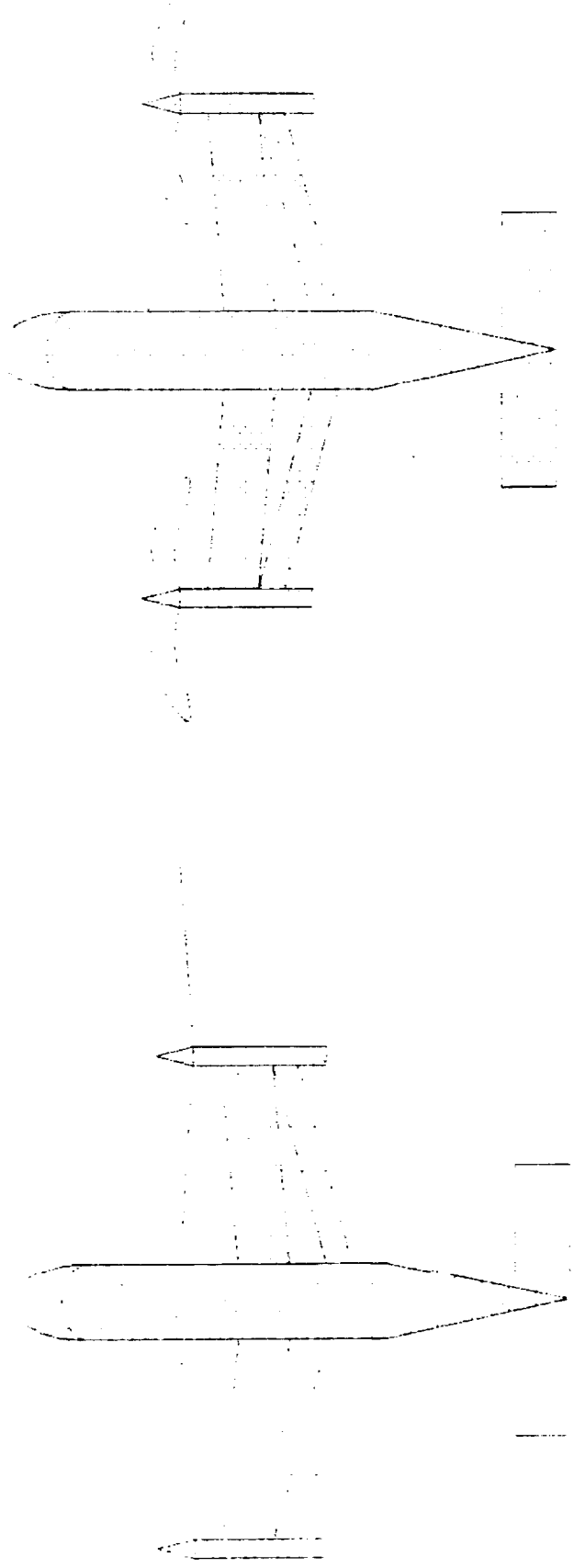

Fig. 28. Tiltrotor VTOL Aircraft

APPENDIX: FINITE-ELEMENT STRUCTURAL MODELS

APPENDIX: FINITE-ELEMENT STRUCTURAL MODELS.

In this Appendix are presented four basic configurations from which any other joined-wing model in this report can be derived. Table A1 shows the weight distribution and the elastic properties for the 166 AL model which has a thickness/chord ratio of 12% on both front and rear wing. Tables A2 and A3 represent models having 15% thickness/chord ratio on the front wing and 12% on the rear wing. The nacelles of the all CL models have the same weight distribution as the XV-15 nacelle. Table A4 describes the 468 AL model, which has +15 degrees sweep on the front wing.

TABLE A1. STRUCTURAL MODEL FOR CASE 166 AL

	density lbs./in	length L, in	dist. den.x L	conc.at X=229.38	conc.at X=334.38	total weight X 2
NACELLE	5.95	105	624.75	467	1052	4287.5
FUSELAGE	11.259	550	6192.45			6192.45
FRONT WING						
node1 - node2	1 - 2	2 - 3	3 - 4	4 - 5		
EIXX	4.3E+08	4.3E+08	4.5E+08	4.7E+08		
EIZZ	1.2E+10	1.3E+10	1.4E+10	1.5E+10		
area, sq.in.	12.91	13.30	14.32	15.48		
length, in	48.75	48.75	48.75	48.75		
density,lb/cu-in	0.2859	0.2859	0.2859	0.2859		
weight, lb.	179.9347	185.3704	199.5867	215.7544		1561.292
REAR WING						
node1 - node2	11 - 12	12 - 13	13 - 14	14 - 15		
EIXX	46330000	46330000	47100000	48670000		
EIZZ	1.8E+09	1.8E+09	1.8E+09	1.8E+09		
area, sq.in.	7.739	7.739	7.862	8.149		
length, in	53.5	53.5	53.5	53.5		
density,lb/cu-in	0.2859	0.2859	0.2859	0.2859		
weight, lb.	118.3730	118.3730	120.2544	124.6442		963.2894
TOTAL AIRPLANE WEIGHT						13004.53

TABLE A2. STRUCTURAL MODEL FOR CASE 266 AL

	density lbs./in	length L, in	dist. den.x L	conc.at X=229.38	conc.at X=334.38	total weight X 2
NACELLE	5.95	105	624.75	467	1052	4287.5
FUSELAGE	11.2597	550	6192.635			6192.835
FRONT WING						
node1 - node2	1 - 2	2 - 3	3 - 4	4 - 5		
EIXX	6.9E+08	6.9E+08	7.2E+08	7.5E+08		
EIZZ	1.2E+10	1.3E+11	1.5E+11	1.6E+10		
area, sq.in.	13.15	13.59	14.58	15.72		
length, in	48.75	48.75	48.75	48.75		
density,lb/cu-in	0.2825	0.2825	0.2825	0.2825		
weight, lb.	181.1001	187.1597	200.7939	216.4938		1571.095
REAR WING						
node1 - node2	11 - 12	12 - 13	13 - 14	14 - 15		
EIXX	46330000	46330000	47100000	48670000		
EIZZ	1.8E+09	1.8E+09	1.8E+09	1.8E+09		
area, sq.in.	7.739	7.739	7.862	8.149		
length, in	53.5	53.5	53.5	53.5		
density,lb/cu-in	0.2825	0.2825	0.2825	0.2825		
weight, lb.	116.9653	116.9653	118.8243	123.1619		951.8337
TOTAL AIRPLANE WEIGHT						13003.26

TABLE A3. STRUCTURAL MODEL FOR CASE 266 CL

	density lbs./in	length L, in	dist. den.x L	conc.at 236.18	conc.at 341.18	total weight X 2
NACELLE	15.1	105	1585.5	558.73		4288.46
FUSELAGE	12.288	505	6205.44			6205.44
FRONT WING						
node1 - node2	1 - 2	2 - 3	3 - 4	4 - 5		
EIXX	6.9E+08	6.9E+08	7.2E+08	7.5E+08		
EIZZ	1.2E+10	1.3E+11	1.5E+11	1.6E+10		
area, sq.in.	13.15	13.59	14.58	15.72		
length, in	48.75	48.75	48.75	48.75		
density,lb/cu-in	0.2825	0.2825	0.2825	0.2825		
weight, lb.	181.1001	187.1597	200.7939	216.4938		1571.095
REAR WING						
node1 - node2	11 - 12	12 - 13	13 - 14	14 - 15		
EIXX	46330000	46330000	47100000	48670000		
EIZZ	1.8E+09	1.8E+09	1.8E+09	1.8E+09		
area, sq.in.	7.739	7.739	7.862	8.149		
length, in	53.5	53.5	53.5	53.5		
density,lb/cu-in	0.2825	0.2825	0.2825	0.2825		
weight, lb.	116.9653	116.9653	118.8243	123.1619		951.8337
TOTAL AIRPLANE WEIGHT						13016.82

TABLE A4. STRUCTURAL MODEL FOR CASE 468 AL

	density lbs./in	length L, in	dist. den.x L	conc.at X=229.38	conc.at X=334.38	total weight X 2
NACELLE	5.95	105	624.75	467	1052	4287.5
FUSELAGE	11.669	533.62	6226.811			6226.811
FRONT WING						
node1 - node2	1 - 2	2 - 3	3 - 4	4 - 5		
EIXX	4.2E+08	4.4E+08	4.7E+08	4.9E+08		
EIZZ	1.1E+10	1.3E+10	1.6E+10	1.9E+10		
area, sq.in.	12.57	14.30	16.63	19.6		
length, in	49.95	49.95	49.95	49.95		
density,lb/cu-in	0.2736	0.2736	0.2736	0.2736		
weight, lb.	171.7856	195.4283	227.2709	267.8598		1724.689
REAR WING						
node1 - node2	11 - 12	12 - 13	13 - 14	14 - 15		
EIXX	39900000	39900000	40670000	42240000		
EIZZ	1.5E+09	1.5E+09	1.5E+09	1.5E+09		
area, sq.in.	6.412	6.412	6.535	6.821		
length, in	53.5	53.5	53.5	53.5		
density,lb/cu-in	0.2736	0.2736	0.2736	0.2736		
weight, lb.	93.85629	93.85629	95.65671	99.84306		766.4247
TOTAL AIRPLANE WEIGHT						13005.42

NASA
National Aeronautics and Space Administration

Report Documentation Page

1. Report No.	2. Government Accession No.	3. Recipient's Catalog No.
NASA CR-177543		

4. Title and Subtitle
Application of the Joined Wing to Tiltrotor Aircraft

5. Report Date
November 1989

6. Performing Organization Code

7. Author(s)
Julian Wolkovitch, Barnaby Wainfan, Yitzhak Ben-Harush,* and Wayne Johnson**

8. Performing Organization Report No.

10. Work Unit No.
505-61-51

9. Performing Organization Name and Address
*ACA Industries, Inc., 28603 Trailriders Drive, Rancho Palos Verdes, CA 90274
**Johnson Aeronautics, P.O. Box 1253, Palo Alto, CA 94302

11. Contract or Grant No.
NAS2-12988

13. Type of Report and Period Covered
Contractor Report

12. Sponsoring Agency Name and Address
National Aeronautics and Space Administration
Washington, DC 20546-0001

14. Sponsoring Agency Code

15. Supplementary Notes
Point of Contact: Ruth Heffernan, Ames Research Center, MS TR-42, Moffett Field, CA 94035-1000
(415) 694-5043 or FTS 464-5043

16. Abstract

A study was made to determine the potential speed improvements and other benefits resulting from the application of the joined wing concept to tiltrotor aircraft. Using the XV-15 as a baseline, the effect of replacing the cantilever wing by a joined-wing pair was studied. The baseline XV-15 cantilever wing has a thickness/chord ratio of 23%. It was found that this wing could be replaced by a joined-wing pair of the same span and total area employing airfoils of 12% thickness/chord ratio. The joined wing meets the same static strength requirements as the cantilever wing, but increases the limiting Mach Number of the aircraft from M = 0.575 to M = 0.75, equivalent to an increase of over 100 knots in maximum speed.

The joined wing configuration studied is lighter than the cantilever and has approximately 11% less wing drag in cruise. Its flutter speed of 245 knots EAS is not high enough to allow the potential Mach number improvement to be attained at low altitude. The flutter speed can be raised either by employing rotors which can be stopped and folded in flight at speeds below 245 knots EAS, or by modifying the airframe to reduce adverse coupling with the rotor dynamics. Several modifications of wing geometry and nacelle mass distribution were investigated, but none produced a flutter speed above 260 knots EAS. It was concluded that additional research is required to achieve a more complete understanding of the mechanism of rotor/wing coupling, and to implement improvements through changes in wing geometry, advanced materials, or rotor modifications.

If the flutter speed can be raised, the research would yield increases in speed of tiltrotor aircraft, enabling such aircraft to combine their vertical takeoff and landing capabilities with cruise speeds equal to those of conventional aircraft.

17. Key Words (Suggested by Author(s))	18. Distribution Statement
Joined wing Tiltrotor Aeroelastic stability Rotor performance	Unclassified-Unlimited Subject Category - 05

19. Security Classif. (of this report)	20. Security Classif. (of this page)	21. No. of Pages	22. Price
Unclassified	Unclassified	99	A05